Electronic Supplementary Material (ESI) for ChemComm.

Supporting Information

Size-selective encapsulation of C_{60} and C_{60}-derivatives within an adaptable naphthalene-based tetragonal prismatic supramolecular nanocapsule

Cristina García-Simón,* Alba Monferrer, Marc Garcia-Borràs, Inhar Imaz, Daniel Maspoch, Miquel Costas,* Xavi Ribas*

Table of contents:

1. Supplementary methods

1.1. Materials and methods

Unless indicated otherwise, reagents and solvents used were commercially available reagent quality.

1.2. Instrumentation

NMR spectra (^{1}H and ^{13}C) were measured on a Bruker DRX 400; $CDCl_3$, CD_3CN or Toluene-d_8 were used as solvents, if not further indicated. High resolution mass spectra (HRMS) were recorded on a Bruker MicroTOF-Q-II, using acetonitrile as the mobile phase. UV-Vis spectroscopy was performed on an Agilent 8452 UV-vis spectrophotometer with 2 mm quartz cell. HPLC data concerning fullerene identity were collected on Agilent series 1200 chromatograph equipped with Cromasil Buckyprep-M column, or LC-9130 NEXT apparatus (Japan Analytical Industry Co. Ltd.) monitored using a UV detector at 320 nm. Toluene as eluent (1 mL/min flow).

1.3. Synthesis of ligand 1c and molecular clip $[Pd\text{-}1c\cdot(AcO)_2]\cdot(CF_3SO_3)_2$

Synthesis of 2,6-bis-hydroxymethyl naphthalene. To an ice-cooled solution of dimethyl naphthalene-2,6-dicarboxylate (3.66 g, 15 mmol) in dry THF (150 ml) under nitrogen, $LiAlH_4$ (2.28 g, 60 mmol) was carefully added. The reaction was allowed to reach room temperature for 40 min, and then was warmed up to 343 K for 3h. The mixture was carefully treated in sequence with 2.3 ml of water, 2.3 ml of a 15% NaOH aqueous solution, and 6.8 ml of water. Afterwards, the suspension was filtered and the solution was evaporated to yield a white solid (2.50 g, 89% yield).[1] ^{1}H-NMR (400 MHz, DMSO): 7.80 (d, J= 8.3Hz, 2H, arom), 7.75 (s, 2H, arom), 7.41 (dd, J= 8.3, 1.3 Hz, 2 H, arom), 5.3 (s, 2H, -OH), 4.62 (d, J= 2.6 Hz, -CH_2-).

Synthesis of naphthalene-2,6-dicarbaldehyde. To a stirred suspension of pyridinium chlorochromate (8.85 g, 41.1 mmol) in anhydrous CH_2Cl_2 (100 ml) at 323 K under nitrogen, a suspension of 2,6-bis-hydroxymethyl naphthalene (2.50 g, 13.6 mmol) in anhydrous CH_2Cl_2 (50 ml) was added in one portion. The reaction mixture was rigorously stirred for 4 h at 323 K, cooled to room temperature and poured into cold diethyl ether (500 ml). The mixture was triturated until the tar solidified and then filtered through a large pad of silica, eluting with an additional portion of ether (200 ml). The solvents were removed by evaporation, water (200 ml) was added, and the resulting solution was extracted with CH_2Cl_2 (3×50 ml) The organic layer was dried over $MgSO_4$ and

evaporated to yield the naphthalene-2,6-dicarbaldehyde as a white solid (1.24 g, 50% yield).[1] ^{1}H-NMR (400 MHz, $CDCl_3$): 10.24 (s, 2H, -CHO), 8.44 (m, arom), 8.15 (dd, J= 8.4, 1.7 Hz, 2H, arom), 8.09 (dd, J= 8.4, 1.7 Hz, 2H, arom).

Synthesis of H2nph. To a solution of naphthalene-2,6-dicarbaldehyde (0.58 g, 3.1 mmol) in CH_2Cl_2 (210 ml) at room temperature, a solution of diethylentriamine (0.33 g, 3.2 mmol) in CH_3OH (210 ml) was added dropwise within 10 h. After the addition was completed, the mixture was stirred for 24 h, the solution was concentrated to about 200 ml by evaporation, and $NaBH_4$ (0.46 g, 12.2 mmol) was added carefully under stirring. After stirring at 323 K for 12 h, the solvent was removed by evaporation, and water (100 ml) was added. The resulting solution was extracted with CH_2Cl_2 (3×50 ml), the organic layer was dried over $MgSO_4$ and dried by evaporation, and then recrystallized in chloroform (4 mL) and toluene to form pale yellow crystals (0.47 g, 58% yield). ^{1}H-NMR (400 MHz, $CDCl_3$): 7.66 (S, 4 H, arom), 7.52 (d, J= 8.3 Hz, 4 H, arom), 7.34 (dd, J= 8.3, 1.5 Hz, 4 H, arom), 3.92 (s, 8 H, -CH_2-), 2.84 (m, 16H, -CH_2-). ^{13}C-NMR (400 MHz, $CDCl_3$) δ ppm: 135.9 (arom), 132.6 (arom), 127.9 (arom), 126.3 (arom), 126.01 (arom), 54.1 (-CH_2- benzylic), 48.9 (-CH_2-), 48.6 (-CH_2-). ESI-MS (m/z): calculated 511.354 and found 511.352 ({H2pnh+H}$^+$).

Synthesis of Me2nph (1c). Formaldehyde (3.14 mL), H_2O (3.14 mL) and formic acid (2.51 ml) were added in sequence over H2nph (0.21 g, 0.4 mmol) in a round-bottom flask at room temperature. The mixture was stirred at 393 K for 12 h and then cooled down to room temperature. The solvent was removed to dryness and the residue was treated with of NaOH 15% (7.85 mL), stirring for 30 min. The resulting solution was extracted with CH_2Cl_2 (3×15 ml), the organic layer was dried over $MgSO_4$, dried by evaporation and then recrystallized in acetone (0.24 g, 68% yield). ^{1}H-NMR (400 MHz, $CDCl_3$): 7.61 (d, J= 8.3 Hz, 4H, arom), 7.51 (s, 4H, arom), 7.30 (dd, J= 8.3, 1.5 Hz, 4H, arom), 3.35 (s, 8H, -CH_2-), 2.56-2.32 (16 H, m, -CH_2-), 2.26 (s, 6H, -NCH_3), 2.14 (s, 12H, -NCH_3). ^{13}C-NMR (400 MHz, $CDCl_3$) δ ppm: 136.3 (arom), 132.5 (arom), 127.5 (arom), 127.4 (arom), 62.8 (-CH_2-benzylic), 54.2 (-CH_2-), 53.9 (-CH_2-), 43.9 (N-CH_3), 42.9 (N-CH_3). ESI-MS (m/z): calculated 595.445 and found 595.447 ({**1c**+H}$^+$).

Synthesis of [Pd-1c·$(AcO)_2$]$(CF_3SO_3)_2$. Ligand **1c** (0.05 g, 0.084 mmols), $Pd(AcO)_2$ (0.04 g, 0.18 mmols) and anhydrous CH_3CN (16.5 ml) were mixed in a round bottom flask. The mixture is refluxed, under nitrogen atmosphere overnight. Afterwards the reaction was cooled down to room temperature and an excess of $NaCF_3SO_3$ salt was added (1 to 4.2 equivalents respect **1c**) and the mixture was stirred vigorously during 6 h. Finally, the reaction mixture was concentrated to a

volume of 2ml under reduced pressure, filtered through Celite© and recrystallized under slow diethyl ether diffusion. Yellow crystalline solid is obtained (0.08 g, 92% yield (major and minor conformers)). ^{1}H-NMR (*isolated major conformer (Figure S17)*, 400 MHz, CD_3CN): 4.26 (d, J= 12.83 Hz, 4H, -CH_2-), 3.54 (m, 4H, -CH_2-), 3.43 (s, 12H, -NCH_3), 3.26 (d, J= 12.83 Hz, 4H, -CH_2-), 3.23 (m, 4H, -CH_2-), 2.42 (d, J= 13.5 Hz, 4H, -CH_2-), 2.26 (d, J= 13.5 Hz, 4H, -CH_2-). ^{13}C-NMR (*isolated major conformer (Figure S24),* 400 MHz, CD_3CN) δ ppm: 177.03 (C=O, AcO), 133.1 (arom), 131.7 (arom), 130.3 (arom), 65.5 (-CH_2-), 60.4 (-CH_2-), 58.3 (-CH_2-), 42.1 (N-CH3), 23.5 (-CH_3, AcO). ESI-MS (m/z): calculated 1075.228 and found 1075.227 ({[**Pd-1c**·$(AcO)_2$](CF_3SO_3)}$^{+}$), calculated 463.138 and found 463.138 ({[**Pd-1c**·$(AcO)_2$]$^{2+}$).

1.4. Synthesis of nanocapsule 5·$(BArF)_8$

Synthesis of nanocapsule 5·$(CF_3SO_3)_8$. 5,10,15,20-tetrakis(4-carboxyphenyl)-porphyrin-Zn(II) (11.02 mg, 0.012 mmol) was weighed in a 10 ml flask and 0.5 ml of DMF were added. Afterwards, triethylamine (11 µl) was dissolved in 0.5 ml of DMF and added to the porphyrin solution. Finally, [**Pd-1c**·$(AcO)_2$]$(CF_3SO_3)_2$ (30 mg, 0.024 mmols, mixture of conformers) was also dissolved in 2 ml of DMF and added to the mixture. The reaction mixture was heated to 105ºC under reflux during 18 h. After the reaction time, the mixture was cooled to room temperature, filtered through Celite© and crystallized by diethyl ether diffusion. The product obtained was a dark purple crystalline material (26.31 mg, 66.0% yield). Low solubility prevented NMR characterization, however, HRMS mass experiments could be performed. HRMS (m/z): calcd. 1381.7464 and found 1381.7506 ({**5**·$(CF_3SO_3)_4$}$^{4+}$); calcd. 1075.6066 and found 1075.6090 ({**5**·$(CF_3SO_3)_3$}$^{5+}$), calcd. 871.5134 and found 871.5149 ({**5**·$(CF_3SO_3)_2$}$^{6+}$); calcd. 725.7332 and found 725.7336 ({**5**·(CF_3SO_3)}$^{7+}$); calcd. 616.2720 and found 616.2716 ({**5**}$^{8+}$).

Synthesis of nanocapsule 5·$(BArF)_8$. **5**·$(CF_3SO_3)_8$ nanocapsule (26.31 mg, 0.004 mmol) was suspended in dichloromethane (20 ml), an excess of NaBArF (38.08 mg, 0.04 mmol, 10 eq.) was added. The mixture was stirred for 12 h at room temperature, and then filtered through a Celite® column. The product was obtained by precipitation using diethyl ether. The dark power obtained was washed several times with diethyl ether to remove the excess of NaBArF. (Yield: 51.93 %). ^{1}H-NMR (400 MHz, CD_3CN): 8.6 (d, J= 7.8 Hz, 8 H, arom-porph), 8.58 (s, 16 H, pyrrole), 8.43 (d, J= 7.8 Hz, 8 H, arom-porph), 8.19 (d, J= 7.8 Hz, 8 H, arom-porph), 7.90 (d, J = 7.8 Hz, arom-porph), 4.21 (J= 12.5, 16H, -CH_2-), 3.69 (m, 16 H, -CH_2-), 3.69 (s, 48 H, -NCH_3), 3.39 (m, 16H, -CH_2-), 3.29 (d, J= 12.3

Hz, 16 H, -CH_2-), 2.52 (d, J= 12.3 Hz, 16 H, -CH_2-), 2.34 (d, J= 11.0 Hz, 16 H, -CH_2-), 1.3 (s, 24 H, -NCH_3). HRMS (m/z): calcd. 2095.8612 and found 2095.8613 ({**5**·$(BArF)_4$}$^{4+}$); calcd. 1503.8755 and found 1503.8754 ({**5**·$(BArF)_3$}$^{5+}$), calcd. 1109.5517 and found 1109.5514 ({**5**·$(BArF)_2$}$^{6+}$); calcd. 827.7490 and found 857.7482 ({**5**·(BArF)}$^{7+}$); calcd. 616.3970 and found 616.3978 ({**5**}$^{8+}$).

1.5. Preparation and characterization of the fullerene adducts.

Preparation of $C_{60}\subset$5·$(BArF)_8$: 1.0 mg of **5**·$(BArF)_8$ nanocapsule (0.085 μmols, 1 equiv.) were dissolved in 100 μl of CH_3CN. Then 1 eq. of C_{60} dissolved in 400 μl of toluene was added to the cage solution. The mixture was stirred at room temperature for 5 minutes. The mixture was filtered and analyzed by HRMS. HRMS (m/z): calcd. 2276.1118 and found 2276.1045 ($\{C_{60}\subset$**5**·$(BArF)_4\}^{4+}$); calcd. 1648.2759 and found 1648.2745 ($\{C_{60}\subset$**5**·$(BArF)_3\}^{5+}$), calcd. 1229.7187 and found 1229.7158 ($\{C_{60}\subset$**5**·$(BArF)_2\}^{6+}$); calcd. 930.6064 and found 930.6032 ($\{C_{60}\subset$**5**·$(BArF)\}^{7+}$); calcd. 706.3972 and found 706.3948 ($\{C_{60}\subset$**5**$\}^{8+}$).

Preparation of $C_{60}\subset$5·$(CF_3SO_3)_8$: 1.0 mg of solid **5**·$(CF_3SO_3)_8$ nanocapsule (0.16 μmols, 1 equiv.) was suspended in a toluene solution of C_{60} (capsule/fullerene ratio was 1/8). The suspension was stirred at room temperature for 48 h. Finally, the mixture was dried under vacuum, redissolved in CH_3CN, filtered and analyzed by HRMS. HRMS (m/z): calcd. 1561.9969 and found 1561.9989 ($\{C_{60}\subset$**5**·$(CF_3SO_3)_4\}^{4+}$); calcd. 1220.0071 and found 1220.0212 ($\{C_{60}\subset$**5**·$(CF_3SO_3)_3\}^{5+}$), calcd. 991.6805 and found 991.6875 ($\{C_{60}\subset$**5**·$(CF_3SO_3)_2\}^{6+}$); calcd. 828.5900 and found 828.5925 ($\{C_{60}\subset$**5**·$(CF_3SO_3)\}^{7+}$); calcd. 706.3972 and found 706.3996 ($\{C_{60}\subset$**5**$\}^{8+}$).

Preparation of $C_{70}\subset$5·$(BArF)_8$: 1.0 mg of **5**·$(BArF)_8$ nanocapsule (0.085 μmols, 1 equiv.) were dissolved in 100 μl of CH_3CN. Then 2 eq. of C_{70} dissolved in 400 μl of toluene was added to the cage solution. The mixture was stirred at room temperature and the reaction was follower over time during 48h. HRMS (m/z): calcd. 2306.1118 and found 2306.0987 ($\{C_{70}\subset$**5**·$(BArF)_4\}^{4+}$); calcd. 1672.2760 and found 1672.2745 ($\{C_{70}\subset$**5**·$(BArF)_3\}^{5+}$), calcd. 1503.8755 and found 1503.8692 ($\{$**5**·$(BArF)_3\}^{5+}$), calcd. 1249.7188 and found 1249.7133 ($\{C_{70}\subset$**5**·$(BArF)_2\}^{6+}$); calcd. 1109.5517 and found 1109.5461 ($\{$**5**·$(BArF)_2\}^{6+}$; calcd. 947.7493 and found 947.7447 ($\{C_{70}\subset$**5**·$(BArF)\}^{7+}$); calcd. 827.7490 and found 827.7449 ($\{$**5**·$(BArF)\}^{7+}$); calcd. 721.3973 and found 721.3944 ($\{C_{70}\subset$**5**$\}^{8+}$) calcd. 616.3970 and found 616.3944 ($\{$**5**$\}^{8+}$).

Preparation of [n-pyrrolidide-C_{60}]$\subset$5·$(BArF)_8$: 1 mg of **5**·$(BArF)_8$ nanocapsule (0.085 μmols, 1 equiv.) were dissolved in 100 μl of CH_3CN. Then 1 eq. of n-pyrrolidide-C_{60} dissolved in 400 μl of toluene was added to the cage solution. The mixture was stirred at room temperature for 5 minutes and analyzed by HRMS. HRMS (m/z): calcd. 2290.3762 and found 2290.3792 ($\{$[N-pyrrolidide-C_{60}]$\subset$**5**·$(BArF)_4\}^{4+}$); calcd. 1659.8876 and found 1659.8888 ($\{$[N-pyrrolidide-C_{60}]$\subset$**5**·$(BArF)_3\}^{5+}$), calcd.

1239.0617 and found 1239.0604 ({[N-pyrrolidide-C_{60}]⊂**5**·$(BArF)_2$}$^{6+}$); calcd. 938.7576 and found 938.7564 ({[N-pyrrolidide-C_{60}]⊂**5**·(BArF)}$^{7+}$); calcd. 713.6545 and found 713.6520 ({[N-pyrrolidide-C_{60}]⊂**5**}$^{8+}$).

Preparation of [PCBM-C_{60}]⊂5·$(BArF)_8$: 1 mg of **5**·$(BArF)_8$ nanocapsule (0.085 µmols, 1 equiv.) were dissolved in 100 µl of CH_3CN. Then 1 eq. of PCBM-C_{60} dissolved in 400 µl of toluene was added to the cage solution. The mixture was stirred at room temperature for 5 minutes and analyzed by HRMS. HRMS (m/z): calcd. 2322.6365 and found 2322.6216 ({[PCBM-C_{60}]⊂**5**·$(BArF)_4$}$^{4+}$); calcd. 1686.0959 and found 1686.0861 ({[PCBM-C_{60}]⊂**5**·$(BArF)_3$}$^{5+}$), calcd. 1261.2353 and found 1261.2284 ({[PCBM-C_{60}]⊂**5**·$(BArF)_2$}$^{6+}$); calcd. 957.9064 and found 957.9027 ({[PCBM-C_{60}]⊂**5**·(BArF)}$^{7+}$); calcd. 730.2843 and found 730.2840 ({[PCBM-C_{60}]⊂**5**}$^{8+}$).

1.6. General procedure for UV-Vis titrations

Host-guest interactions in solution were studied by UV-Vis spectroscopy. Solutions of nanocapsule **5**·$(BArF)_8$ ($6.46\cdot10^{-6}$ M) and of the different fullerenes and fullerene derivatives tested ($1.04\cdot10^{-4}$M) were prepared using CH_3CN/TL (1/9) as solvent. An increasing number of substrate equivalents were added to the nanocapsule solution (0.5 ml, in a 2 mm cuvette cell). The host concentration was kept constant. The stoichiometry of the complexes was studied by fitting the data to a 1:1 UV-vis model using the supramolecular.org software (Online tools for supramolecular chemistry research and analysis. OpenDataFit, Pall Thordarson, CBNS & UNSW. Patron: Sir Fraser Stoddart).

1.7. Diffusion-Ordered NMR spectroscopy experiments

Diffusion-Ordered NMR experiment (DOSY NMR) of **5**·$(BArF)_8$, allows the determination of the translational self-diffusion coefficients (*D*) for these species in acetonitrile solution. Making use of the Stokes-Einstein equation (SEq.1), the hydrodynamic radii (r_H) for the diffused species can be calculated from the *D* value.[2]

$$= \frac{k \cdot T}{6 \cdot \pi \cdot \eta \cdot r_H} \qquad \text{(SEq.1)}$$

where k is the Boltzmann constant, T is the temperature, and η is the viscosity of the solvent (η (CH_3CN) = 0.35 mPa s).

1.8. Molecular Dynamics (MD) simulations

Molecular Dynamics simulations were performed using the GPU code (*pmemd*)[3] of the AMBER 16 package.[4] Parameters for fullerenes and acetonitrile (solvent) were generated within the *antechamber* module using the general AMBER force field (*gaff*),[5] with partial charges set to fit the electrostatic potential generated at the HF/6-31G(d) level by the RESP model.[6] The charges were calculated according to the Merz–Singh–Kollman scheme[7,8] using the Gaussian 09 package.[9] Parameters for supramolecular metallo-cages were generated using the MCPB.py[10] module included in AmberTools16.[4] Each host-guest system was immersed in a pre-equilibrated truncated octahedron box with a 12 Å buffer of acetonitrile molecules using the *leap* module, resulting in the addition of around 750 solvent molecules. The systems were neutralized by addition of explicit counter ions (Cl^-). All subsequent calculations were done using the Stony Brook modification of the Amber14 force field (*ff14sb*).[11] A two-stage geometry optimization approach was performed. The first stage minimizes the positions of solvent molecules and ions imposing positional restraints on the solute by a harmonic potential with a force constant of 500 kcal·mol^{-1}·Å^{-2} and the second stage minimizes all the atoms in the simulation cell except those involved in the harmonic distance restraint. The systems were gently heated using six 50 ps steps, incrementing the temperature by 50 K for each step (0–300 K) under constant-volume and periodic-boundary conditions. Long-range electrostatic effects were modelled using the particle-mesh-Ewald method.[12] An 8 Å cutoff was applied to Lennard–Jones and electrostatic interactions. Harmonic restraints of 30 kcal·mol^{-1} were applied to the solute and the Andersen equilibration scheme was used to control and equalize the temperature. The time step was kept at 1 fs during the heating stages, allowing potential inhomogeneities to self-adjust. Each system was then equilibrated for 2 ns with a 2 fs time step at a constant volume. Production trajectories were then run for an additional 500 ns under the same simulation conditions.

1.9. X-ray Diffraction studies

Crystals of complexes **Pd-1c**·$(AcO)_4$ were grown from slow diffusion of ethyl ether in a CH_3CN solution. The measurement was carried out on a BRUKER SMART APEX CCD diffractometer using graphite-monochromated Mo Kα radiation (λ = 0.71073 Å) from an x-Ray Tube. Crystal data is found in Table S1. Programs used: data collection, Smart version 5.631 (Bruker AXS 1997-02); data reduction, Saint + version 6.36A (Bruker AXS 2001); absorption correction, SADABS version 2.10 (Bruker AXS 2001). Structure solution and refinement was done using SHELXTL Version 6.14

(Bruker AXS 2000-2003). The structure was solved by direct methods and refined by full-matrix least-squares methods on F2. The non-hydrogen atoms were refined anisotropically.

Crystallographic data for **5**·$(CF_3SO_3)_8$, were collected at the XALOC beamline of the ALBA synchrotron at 100 K using a MD2M single-axis diffractometer (Maatel, France) and a Pilatus 6 M detector (Dectris, Switzerland) (λ = 0.69873 Å). Due to their sensitivity to solvent loss, crystals of the complex were mounted in thin glass capillaries and cryopreserved at 100 K. Rapid handling prior to flash cooling in the cryostream was required to collect data. Despite these measures and the use of high intensity synchrotron radiation, few reflections at greater than 2.5 Å resolution were observed. This poor density and fast degradation is attributed to the high symmetry, solvent loss and severe motions of the solvents (volatile ether) and counteranion molecules CF_3SO_3 in the large cavities of the crystal lattice. Nevertheless, the quality of the data was sufficient to establish the connectivity of the structure and the handedness of each metal centre. The structure was solved by charge flipping method using the code Superflip[13] and refined by the full matrix least-squares based of F^2 using SHELX97.[14] Due to the low resolution, bond lengths and angles within pairs of organic ligands were restrained to be similar to each other (SAME), and thermal parameter restraints (SIMU, DELU, RIGU) were applied to all non-metal atoms to facilitate anisotropic refinement. Ligand-based atoms that still displayed thermal parameters greater than 0.5 were further refined to approximate isotropic behaviour (ISOR). Despite numerous attempts at modelling, including with multiple rigid bodies, the counteranions and solvents molecules in the crystal structure could not be precisely located in the difference maps, due to their high thermal disorder. Thus, the counteranions and solvent molecules were omitted by Squeeze program, and the Squeeze results were appended to the CIF file. The SQUEEZEd portion of the structure totals 3278 electrons per unit cell, corresponding to a solvent accessible void of 46,883 $Å^3$ per unit cell. This electron number equates to 8 CF_3SO_3 anions and 26 molecules of DMF (each with 40 electrons) for each individual molecule of **5**·$(CF_3SO_3)_8$, where Z = 2.

2. Supplementary Figures

Figure S1 Schematic representation for the synthesis of **1c** ligand.

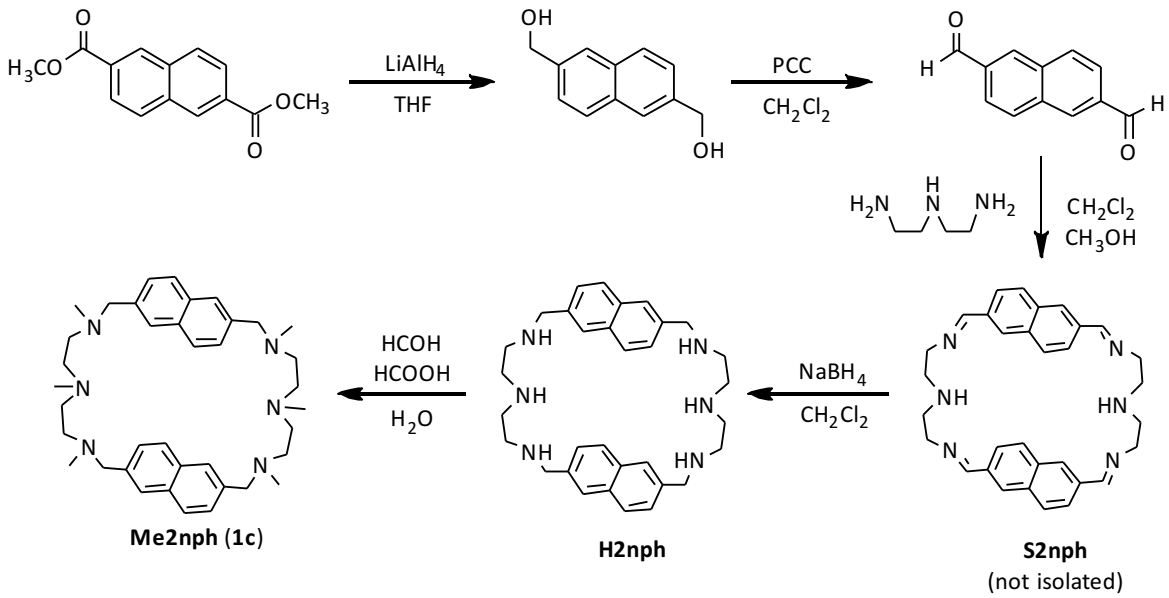

Figure S2. ^{1}H-NMR spectrum of 2,6-bis-hydroxymethyl naphthalene ($CDCl_3$, 298 K, 400 MHz).

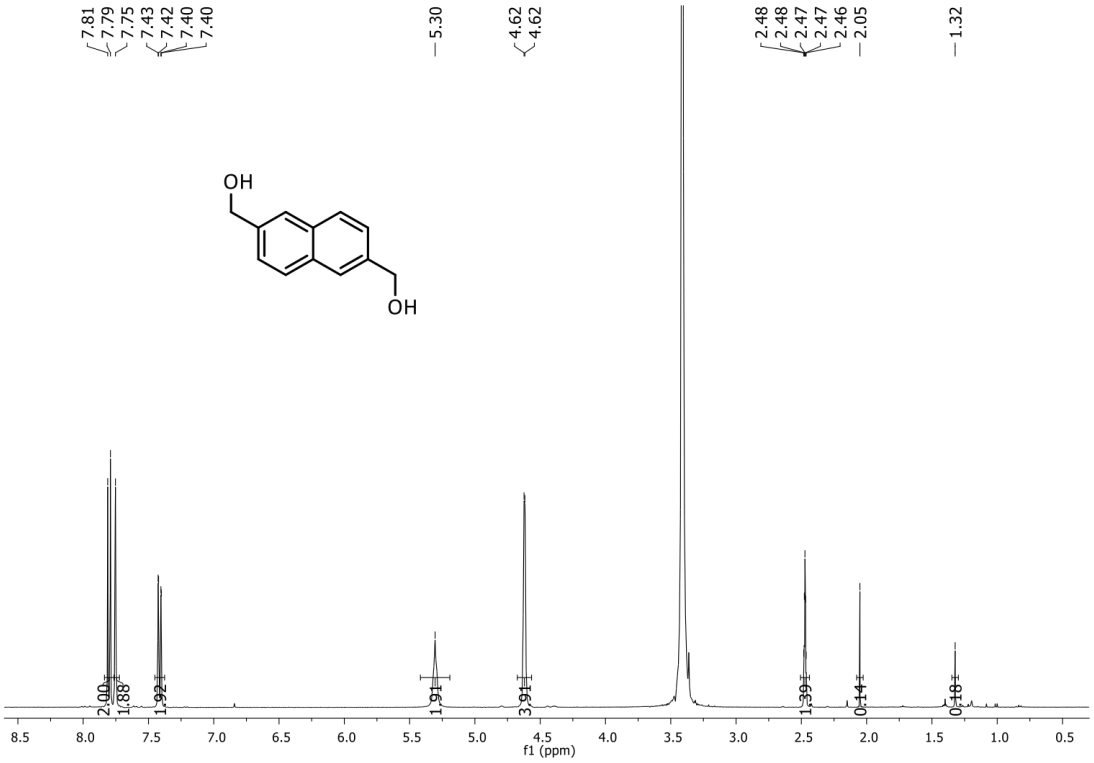

Figure S3. ^{1}H-NRM spectrum of 2,6-bis-methylaldehyde naphthalene ($CDCl_3$, 298 K, 400 MHz).

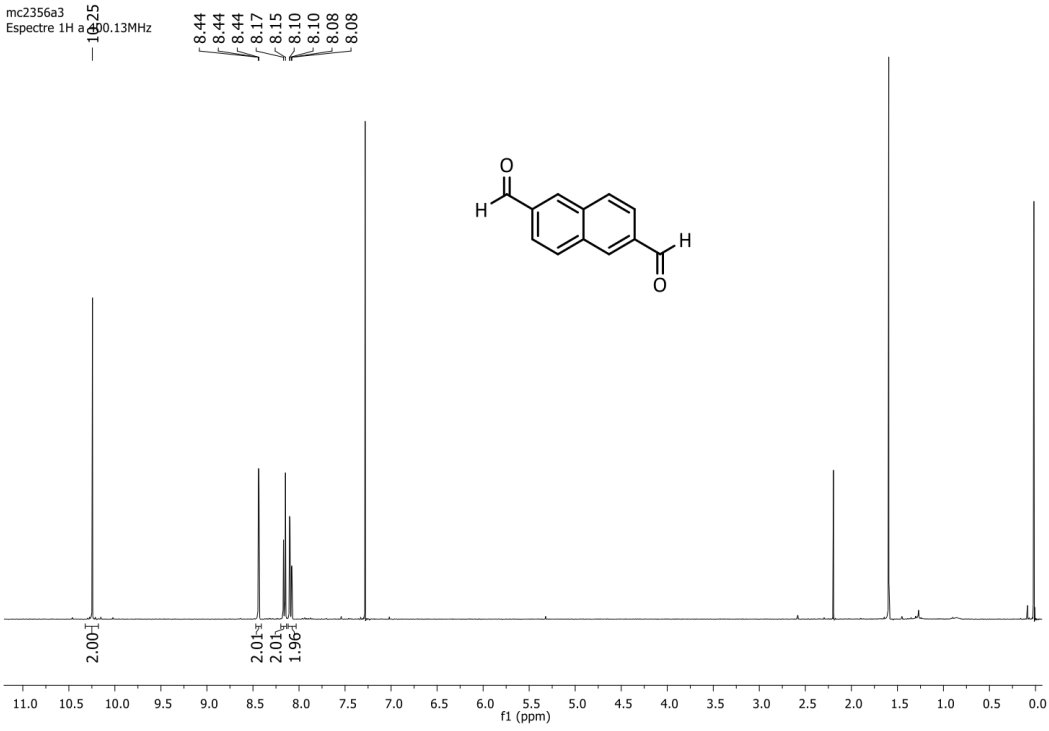

Figure S4. ^{1}H-NRM spectrum of **H2nph** macrocyclic ligand ($CDCl_3$, 298 K, 400 MHz).

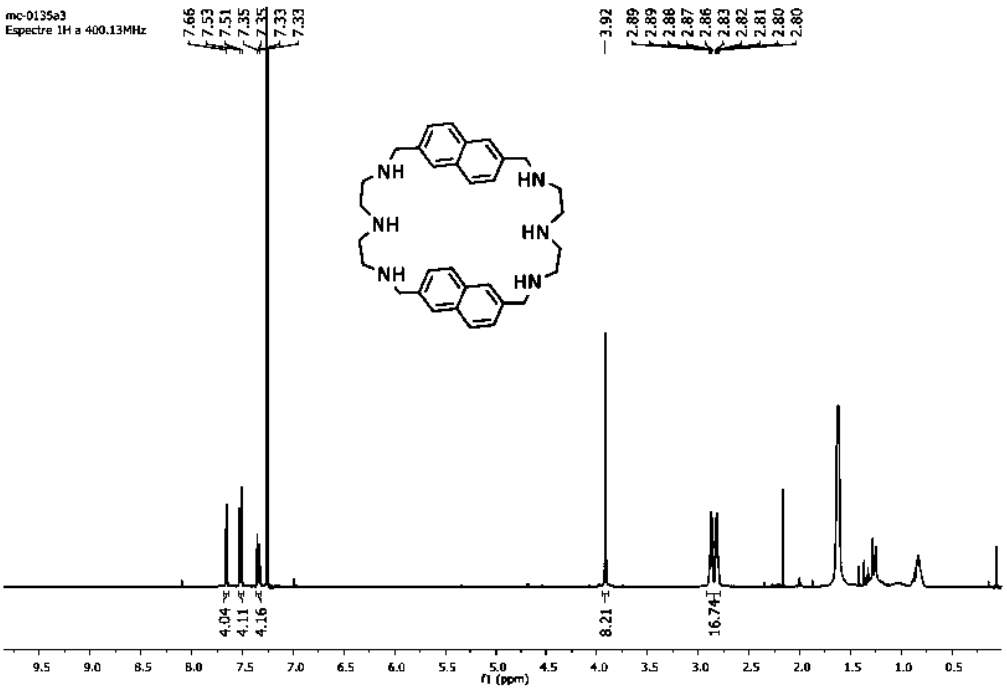

Figure S5. COSY-NMR spectrum of **H2nph** macrocyclic ligand ($CDCl_3$, 298 K, 400 MHz).

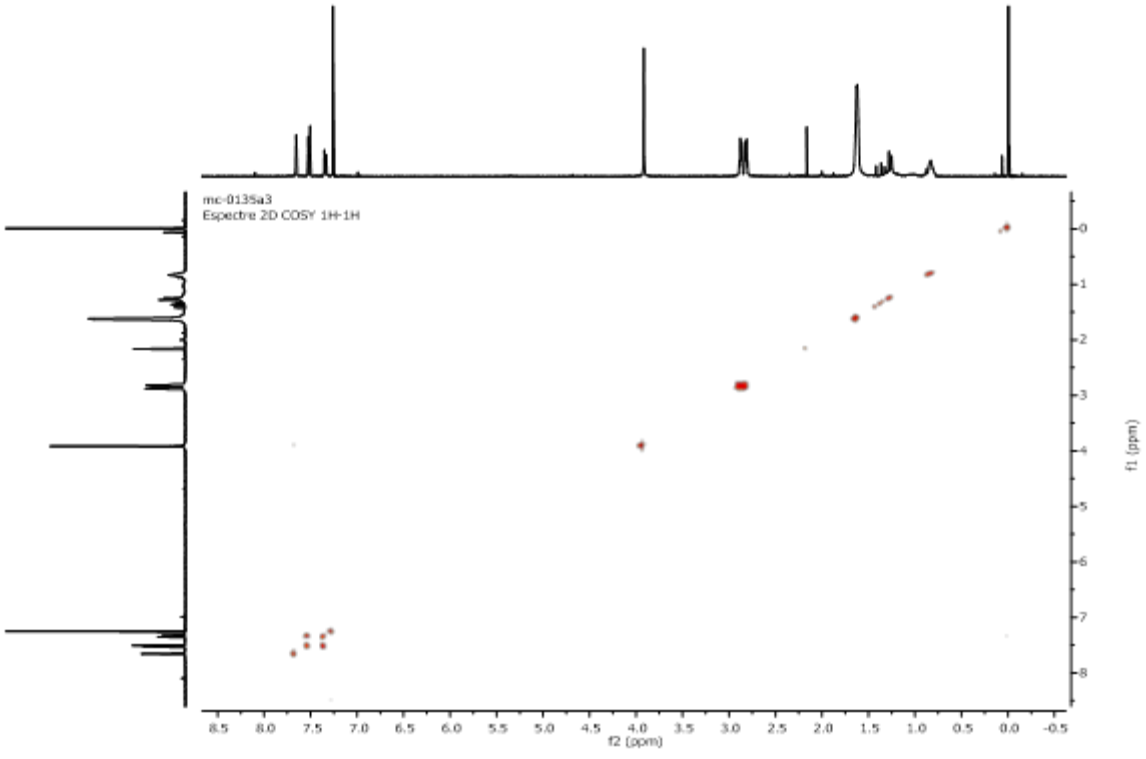

Figure S6. NOESY-NMR spectrum of **H2nph** macrocyclic ligand ($CDCl_3$, 298 K, 400 MHz).

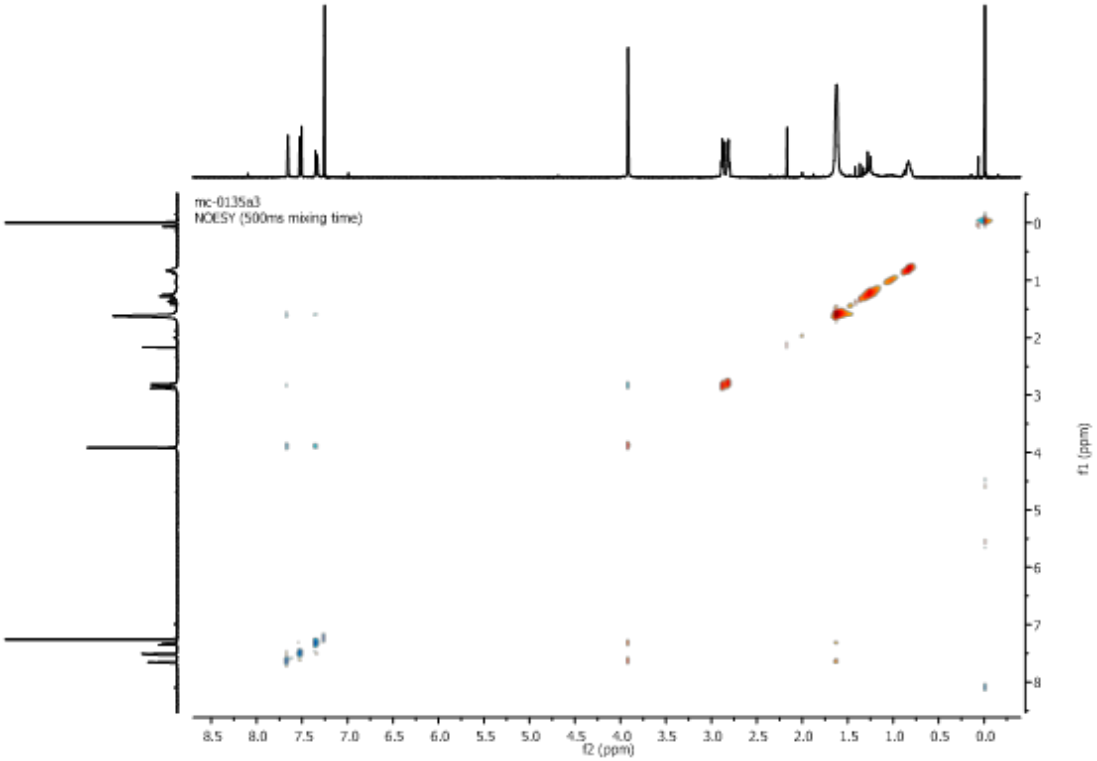

Figure S7. ^{13}C-NMR spectrum of **H2nph** macrocyclic ligand ($CDCl_3$, 298 K, 400 MHz).

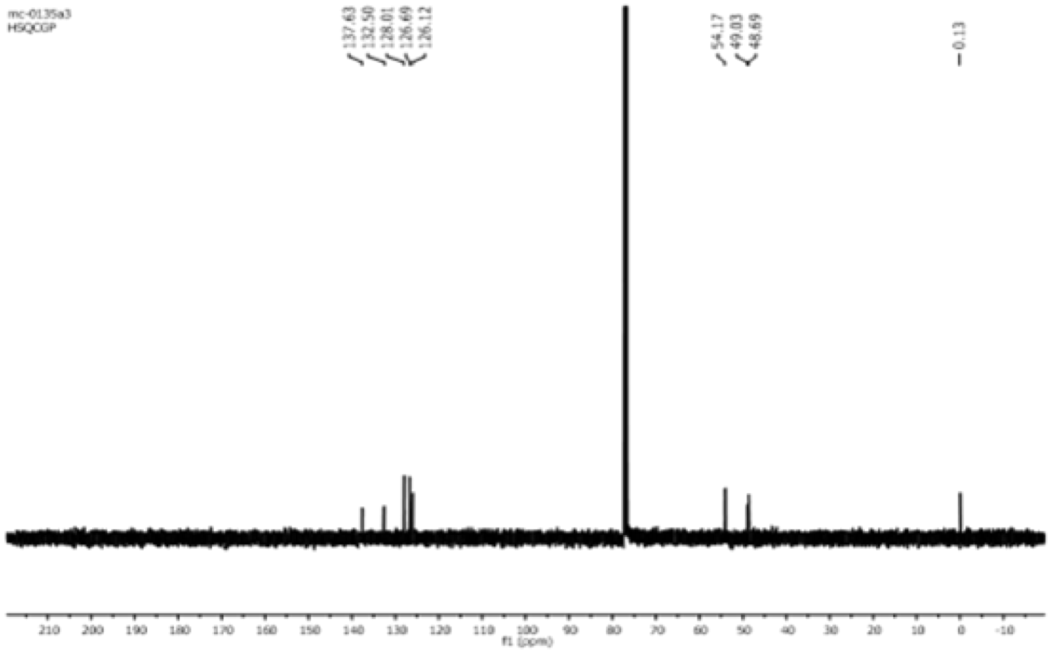

Figure S8. HSQCed-NMR spectrum of **H2nph** macrocyclic ligand ($CDCl_3$, 298 K, 400 MHz).

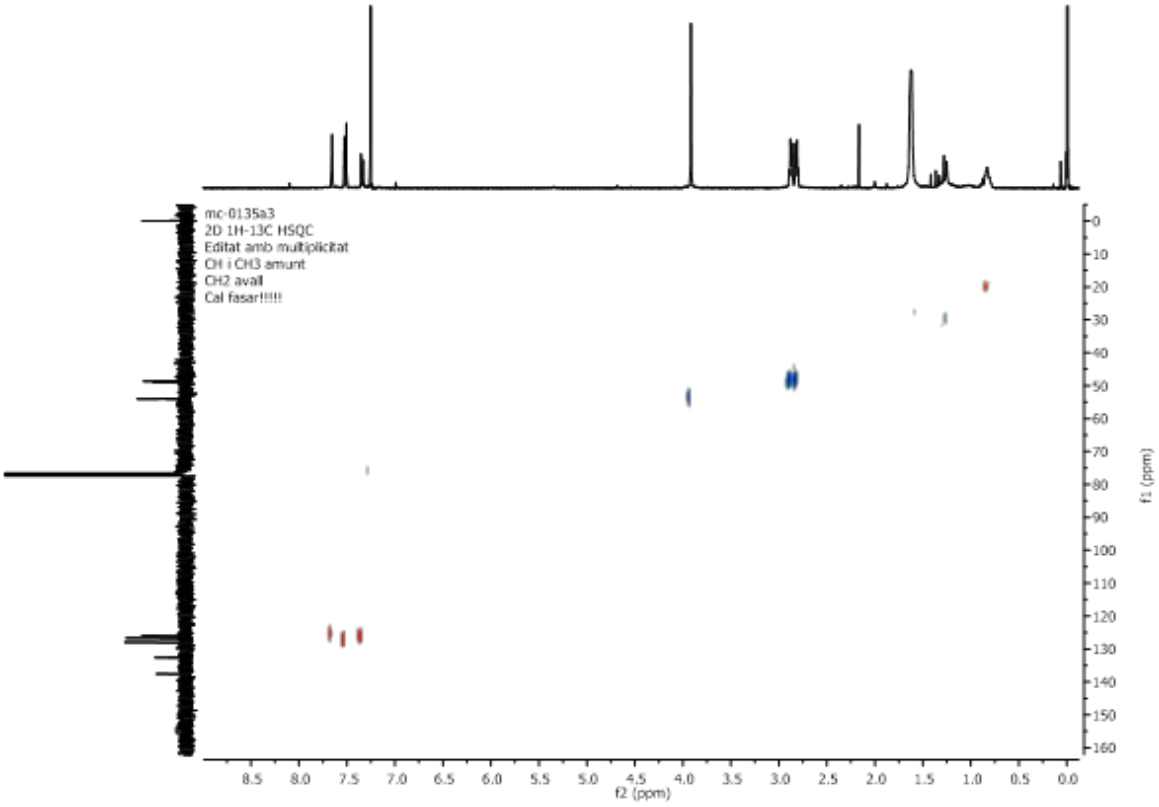

Figure S9. ESI-MS spectrum of the **H2nph** macrocycle. Insert: *top*- found peak, *bottom*- simulated peak pattern.

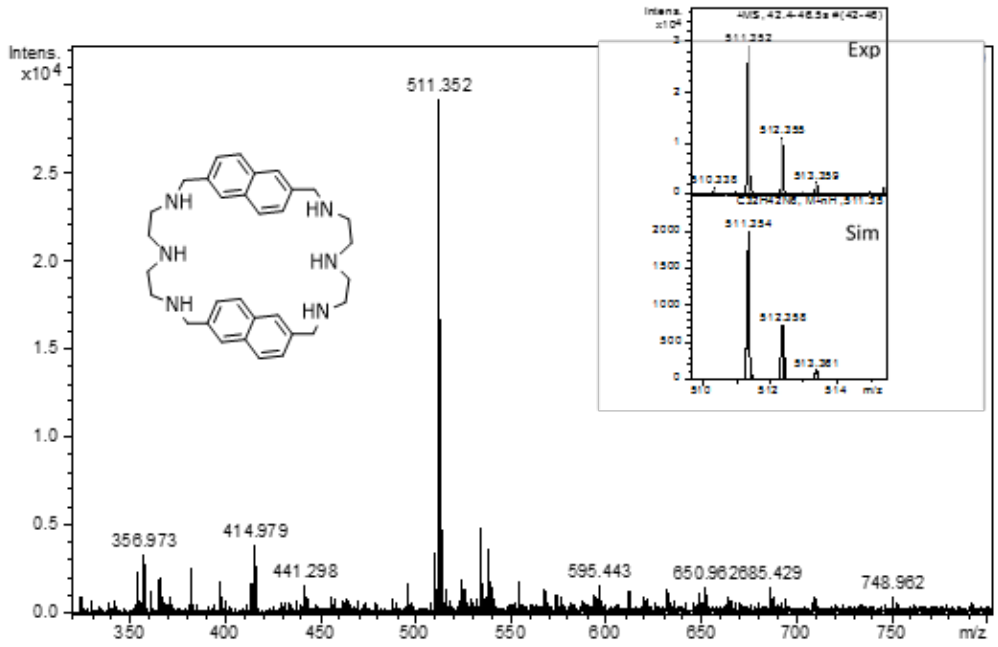

Figure S10. ^{1}H-NRM spectrum of **1c** macrocyclic ligand ($CDCl_3$, 298 K, 400 MHz).

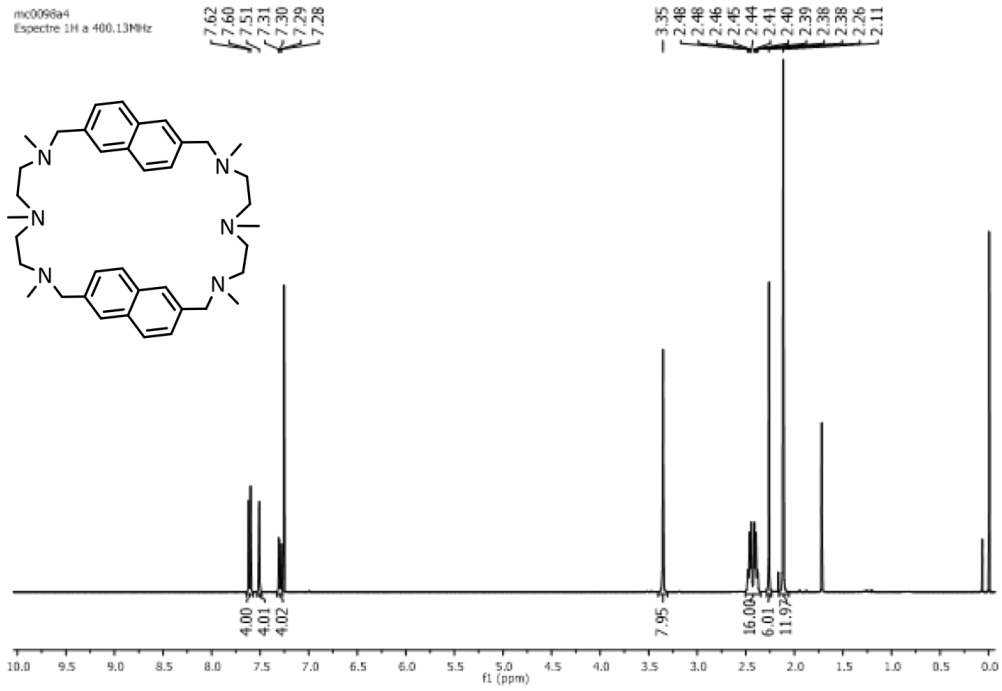

Figure S11. COSY-NMR spectrum of **1c** macrocyclic ligand ($CDCl_3$, 298 K, 400 MHz).

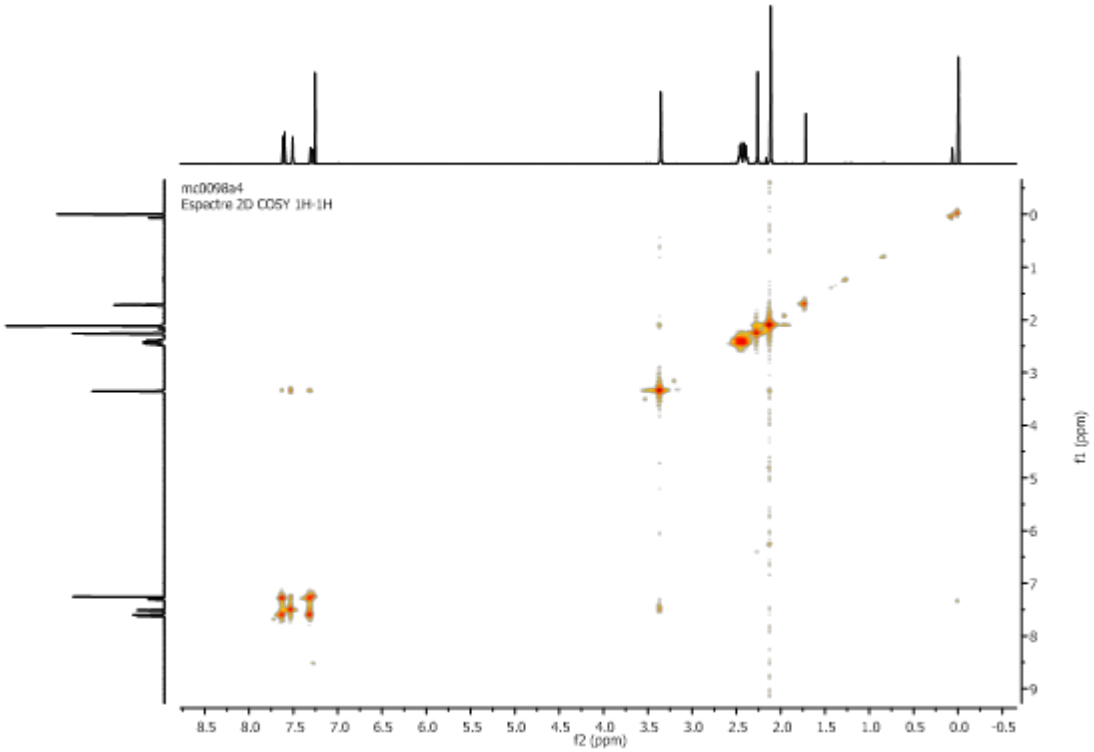

Figure S12. NOESY-NMR spectrum of **1c** macrocyclic ligand ($CDCl_3$, 298 K, 400 MHz).

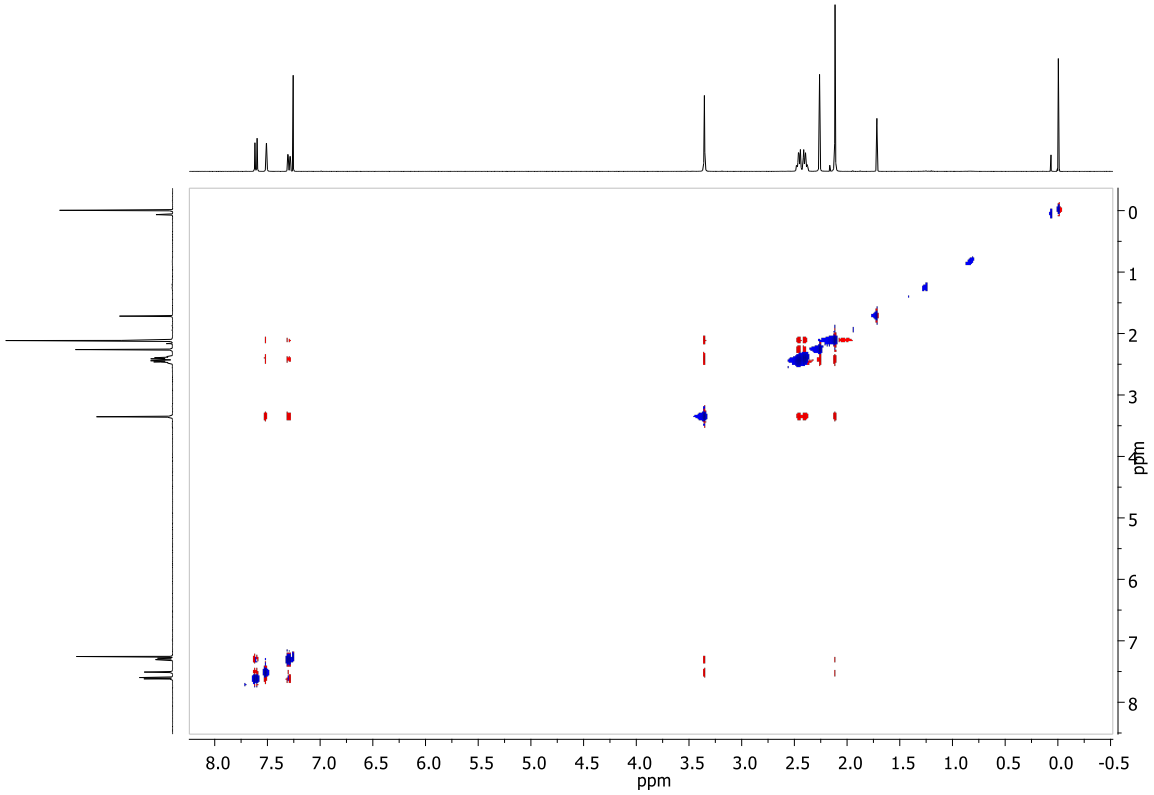

Figure S13. ^{13}C-NMR spectrum of **1c** macrocyclic ligand ($CDCl_3$, 298 K, 400 MHz).

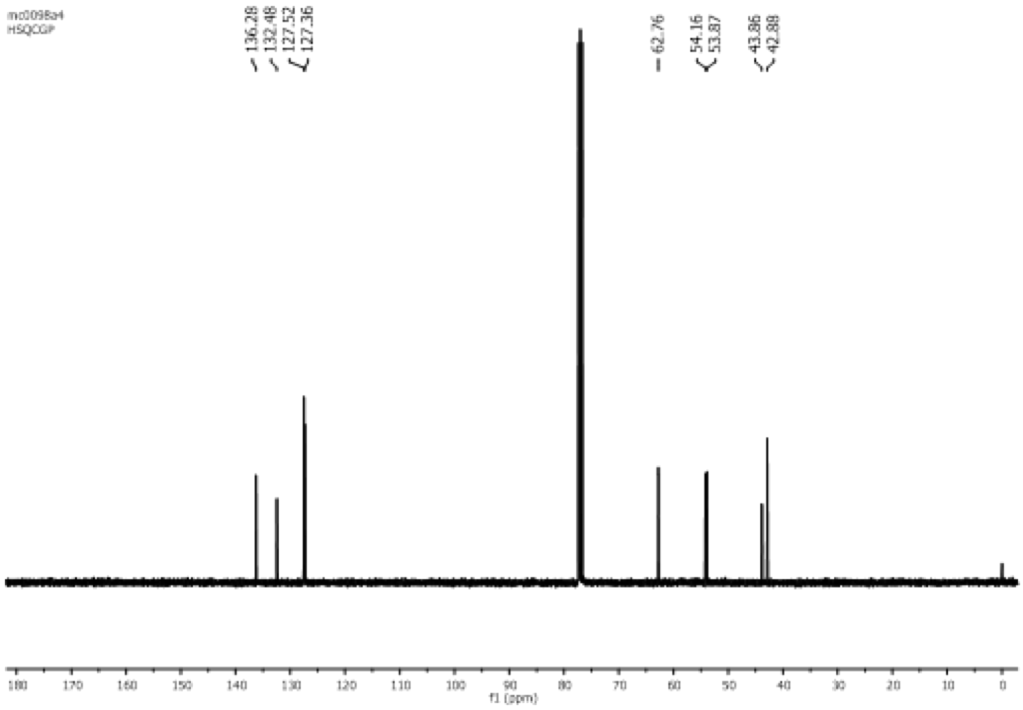

Figure S14. HSQCed-NMR spectrum of **1c** macrocyclic ligand ($CDCl_3$, 298 K, 400 MHz).

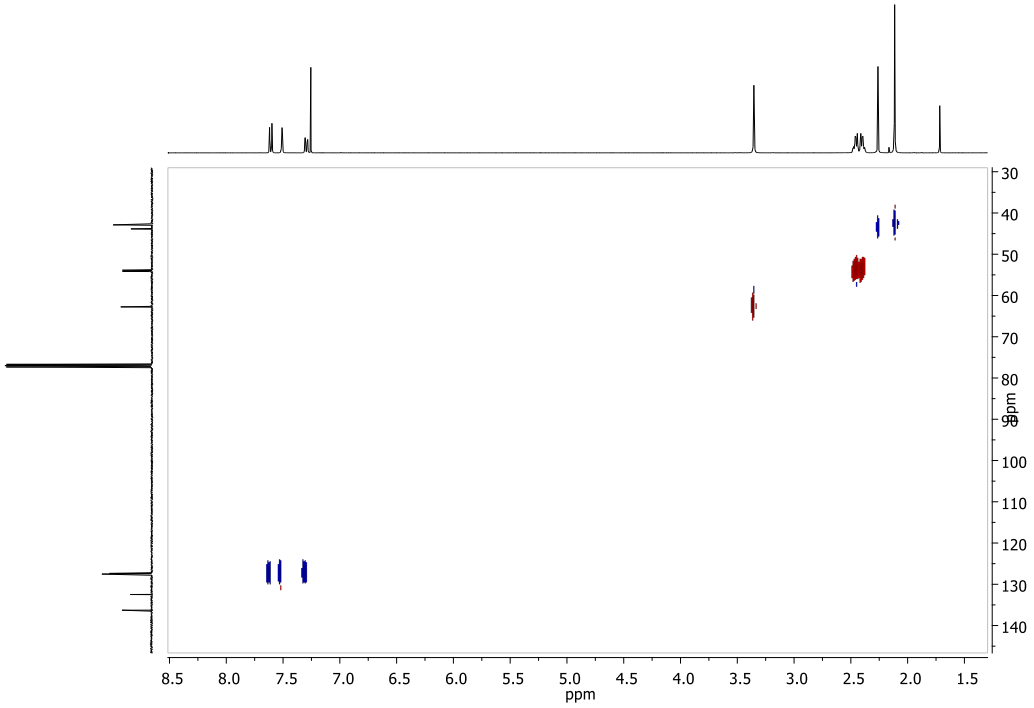

Figure S15. ESI-MS spectrum of **1c** macrocycle. Insert: *top*- found peak, *bottom*- simulated peak pattern.

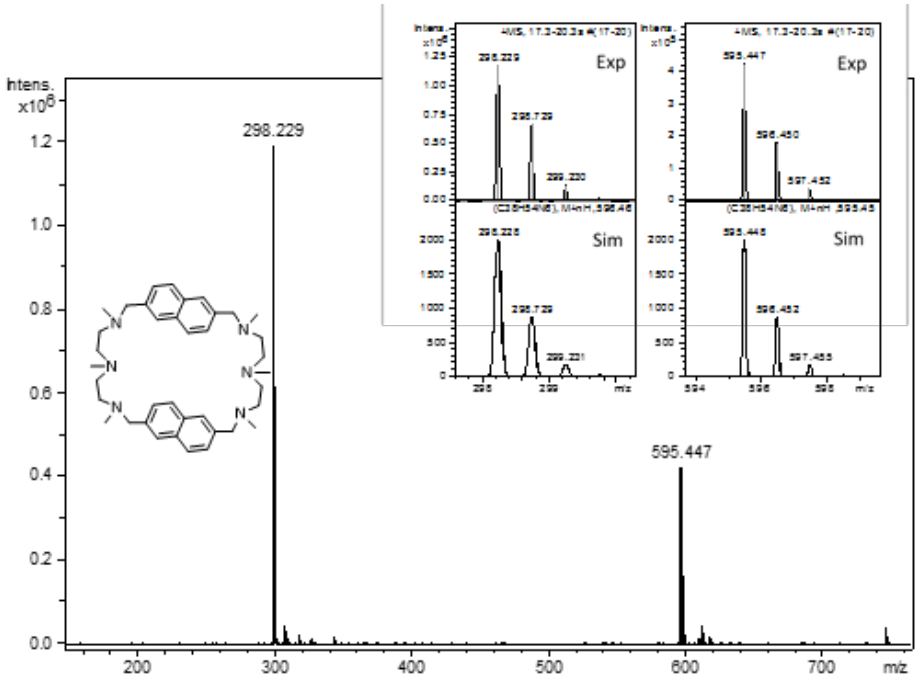

Figure S16. ^{1}H-NMR spectra of [**Pd-1c**·$(AcO)_2$]$(CF_3SO_3)_2$ (mixture of conformers) at **(a)** 328, **(b)** 298, and **(c)** 250 K (CD_3CN). (*)= Internal Standard (Mesitylene).

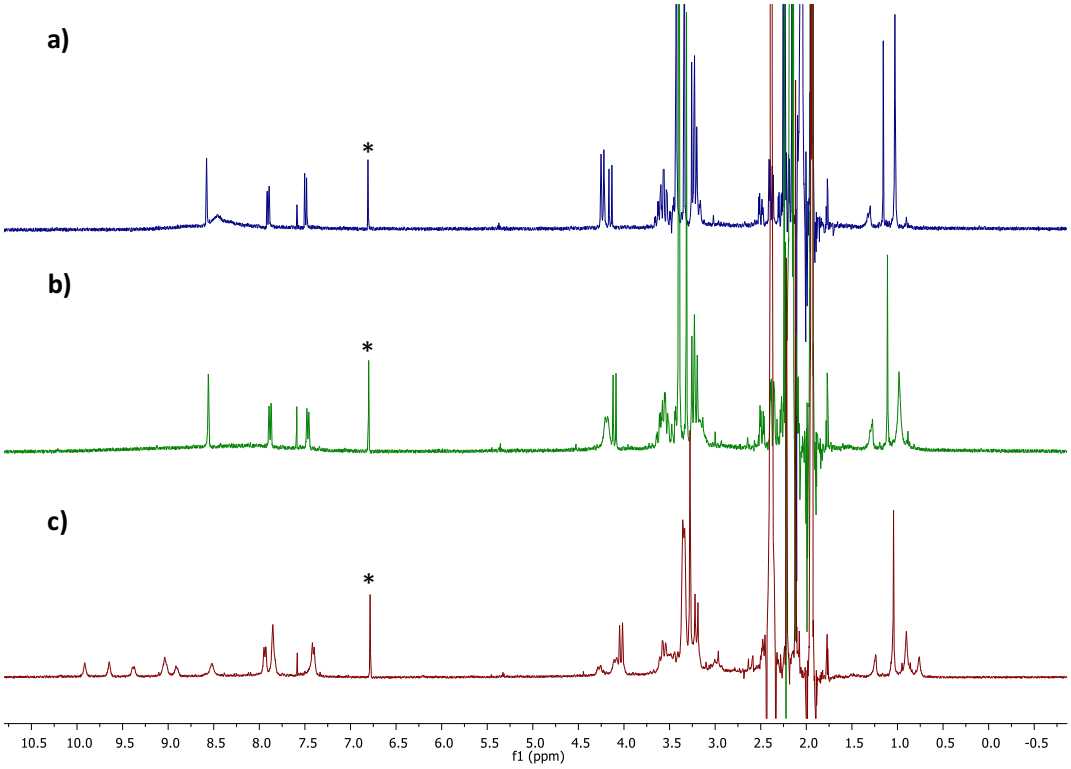

Analogously to molecular clip **Pb-1b**, molecular clip **Pd-1c** displays two conformational isomers in acetonitrile solution. Two separate sets of signals can be observed on the ^{1}H-NMR at different temperatures (Figure S16). One of the conformers displays very broad signals on the aromatic region, most likely due to conformational fluxionality, consequently at low temperature the dynamicity is restricted and the signals become sharper. The other conformational isomer presents sharp signals at all temperatures. Complete exchange to a sole isomer does not occur under the different NMR conditions. Partial crystallization of the reaction mixture lead to the formation of crystals corresponding to a single conformer (the one with broad signals on the aromatic region, see Figure S17), however in the remaining supernatant both isomers were still present. In order to make sure both isomers were suitable to synthetize capsule **5**, two experiments were performed: a) capsule synthetized using the pure conformational isomer obtained by partial recrystallization and b) capsule synthetized using the mixture of isomers obtained from the reaction mixture. Both experiments gave equivalents yields and both leaded to the clean formation of supramolecular capsule **5** strongly suggesting that in the reaction conditions necessary to synthetize the capsule, both conformers of the molecular clip can adopt in solution the right conformation to facilitate self-assembly.

Figure S17. ^{1}H-NMR spectrum of the [**Pd-1c**·$(AcO)_2$]$(CF_3SO_3)_2$ molecular clip (isolated major conformer*), (CD_3CN, 328 K, 400 MHz). (* The major conformer was isolated by crystallization by ether diffusion on acetonitrile solution).

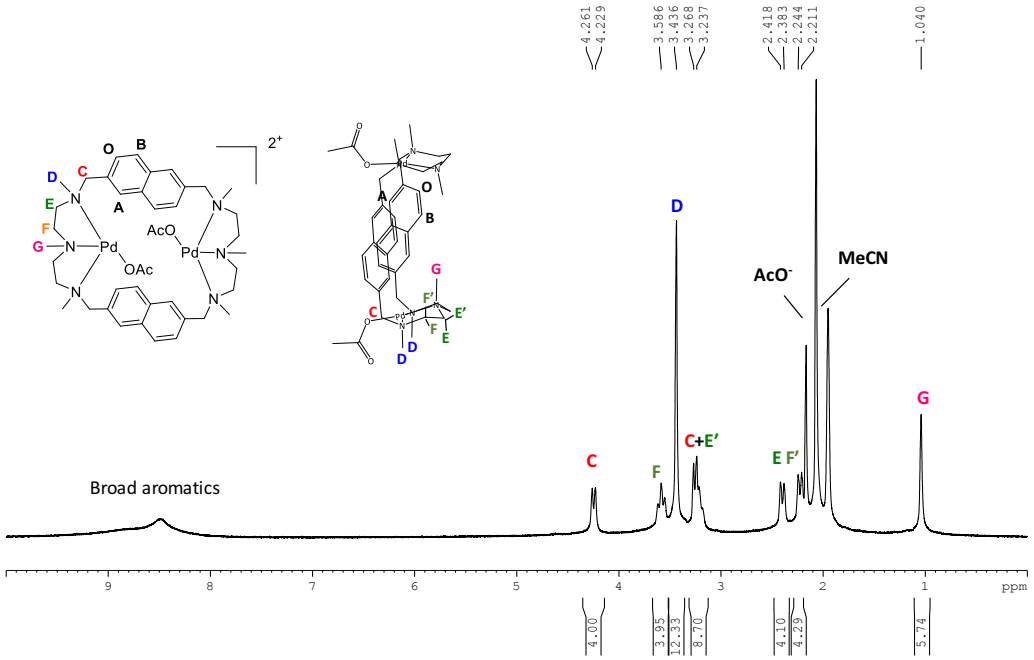

Figure S18. COSY-NMR spectrum of the [**Pd-1c**·$(AcO)_2$]$(CF_3SO_3)_2$ molecular clip (conformer mixture), (CD_3CN, 328 K, 400 MHz).

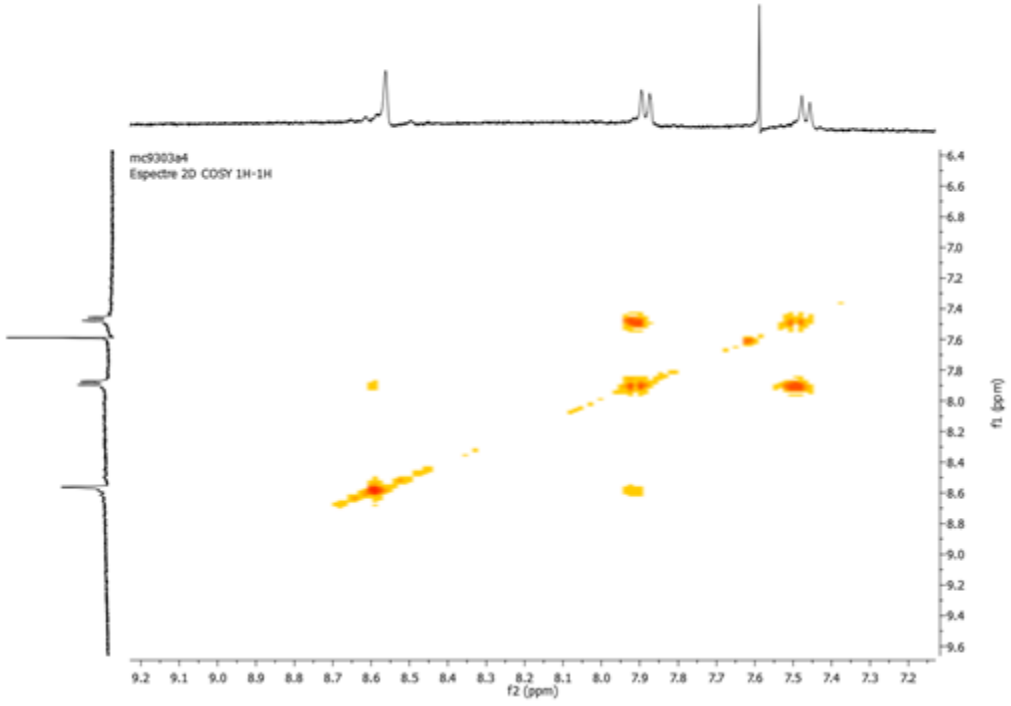

Figure S19. NOESY-NMR spectrum of the [**Pd-1c**·$(AcO)_2$]$(CF_3SO_3)_2$ molecular clip (conformers mixture), (CD_3CN, 328 K, 400 MHz).

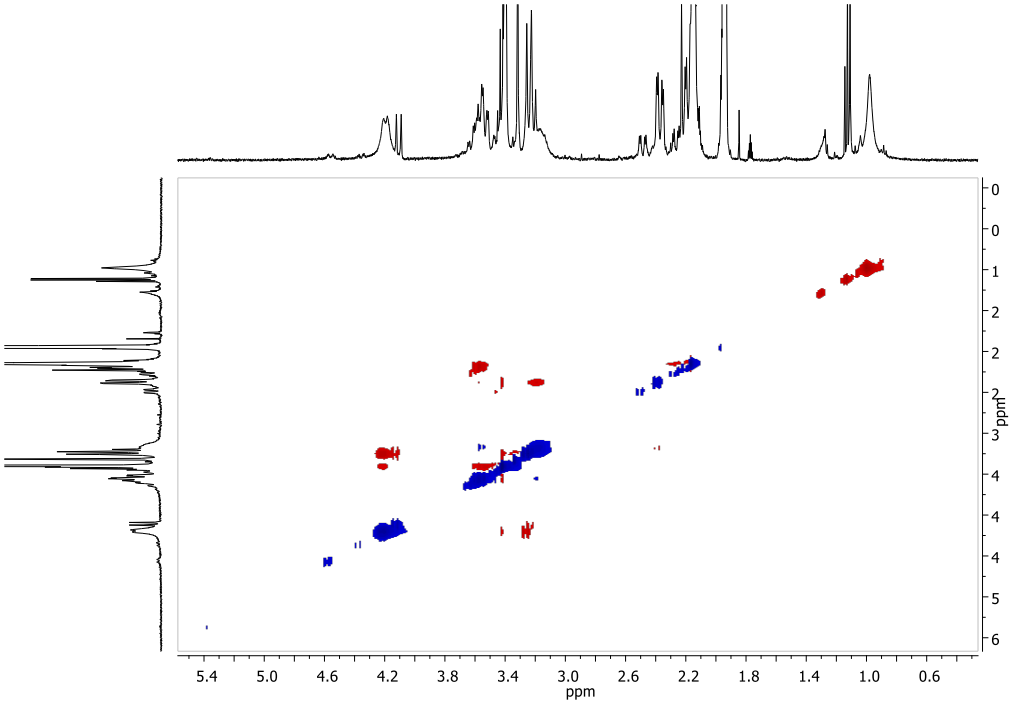

Figure S20. HSQCed-NMR spectrum of the [**Pd-1c**·$(AcO)_2$]$(CF_3SO_3)_2$ molecular clip (conformers mixture), (CD_3CN, 328 K, 400 MHz).

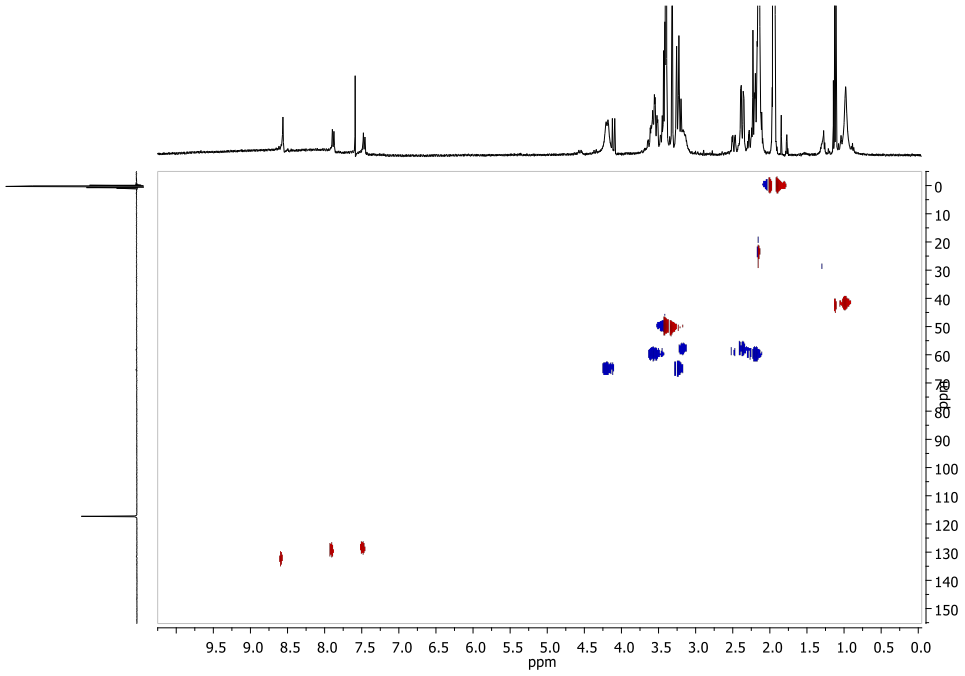

Figure S21. COSY-NMR spectrum of the [**Pd-1c**·$(AcO)_2$]$(CF_3SO_3)_2$ molecular clip (isolated major conformer), (CD_3CN, 328 K, 400 MHz).

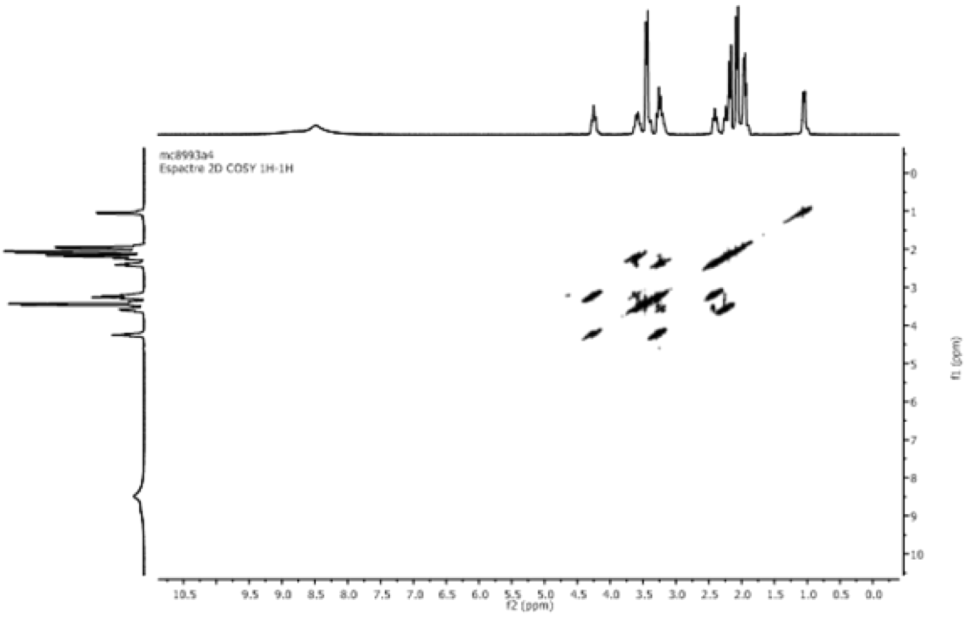

Figure S22. NOESY-NMR spectrum of the [**Pd-1c**·$(AcO)_2$]$(CF_3SO_3)_2$ molecular clip (isolated major conformer), (CD_3CN, 328 K, 400 MHz).

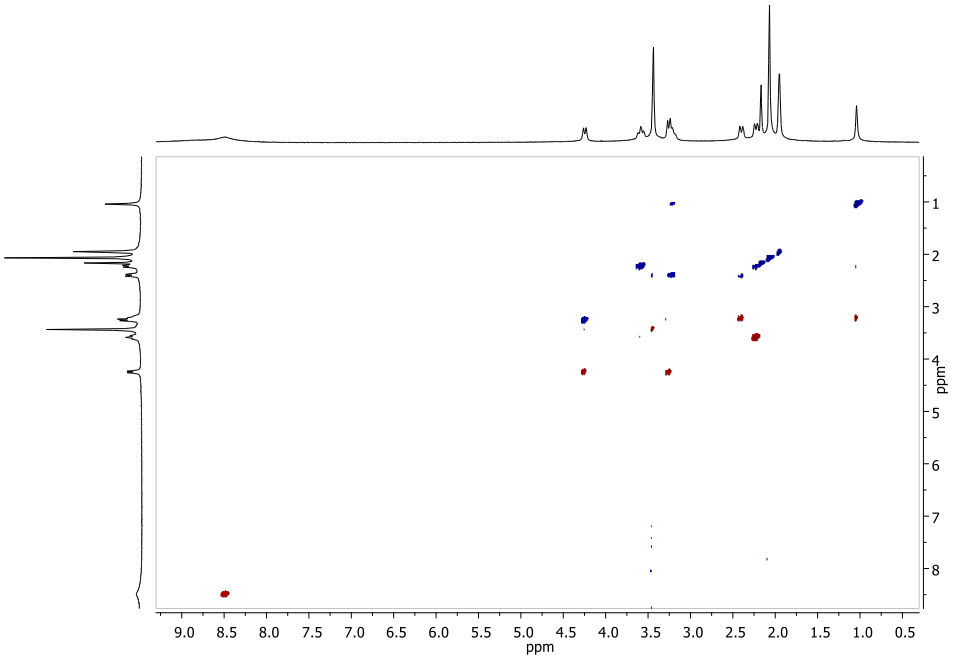

Figure S23. ^{13}C-NMR spectrum of the [**Pd-1c**·$(AcO)_2$]$(CF_3SO_3)_2$ molecular clip (isolated major conformer), (CD_3CN, 328 K, 400 MHz).

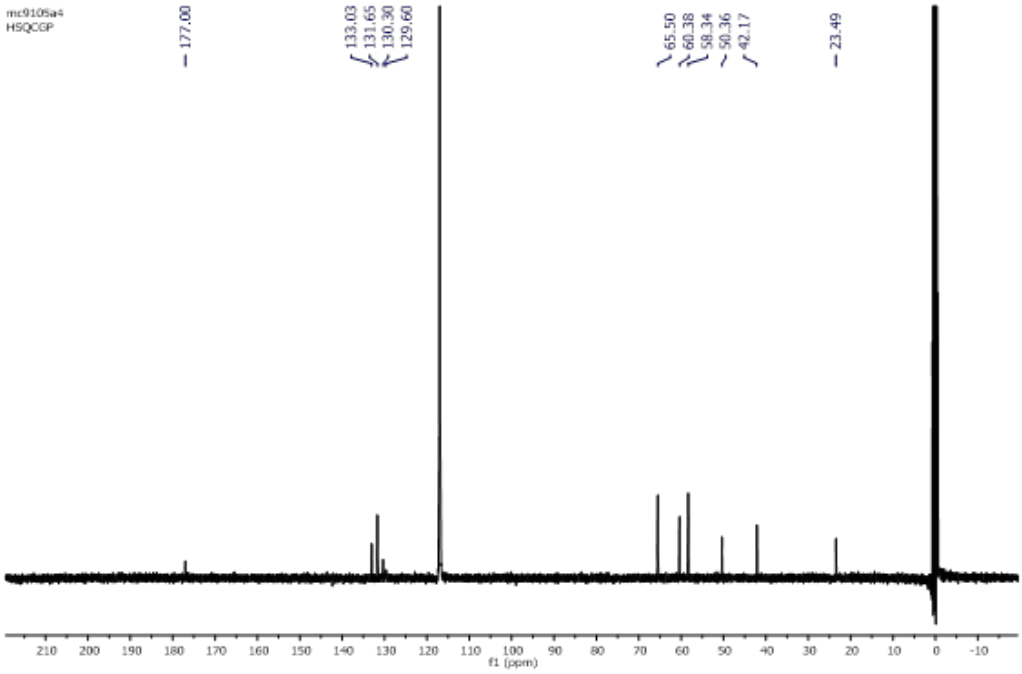

Figure S24. HSQCed-NMR spectrum of the [**Pd-1c**·$(AcO)_2$]$(CF_3SO_3)_2$ molecular clip (isolated major conformer), (CD_3CN, 328 K, 400 MHz).

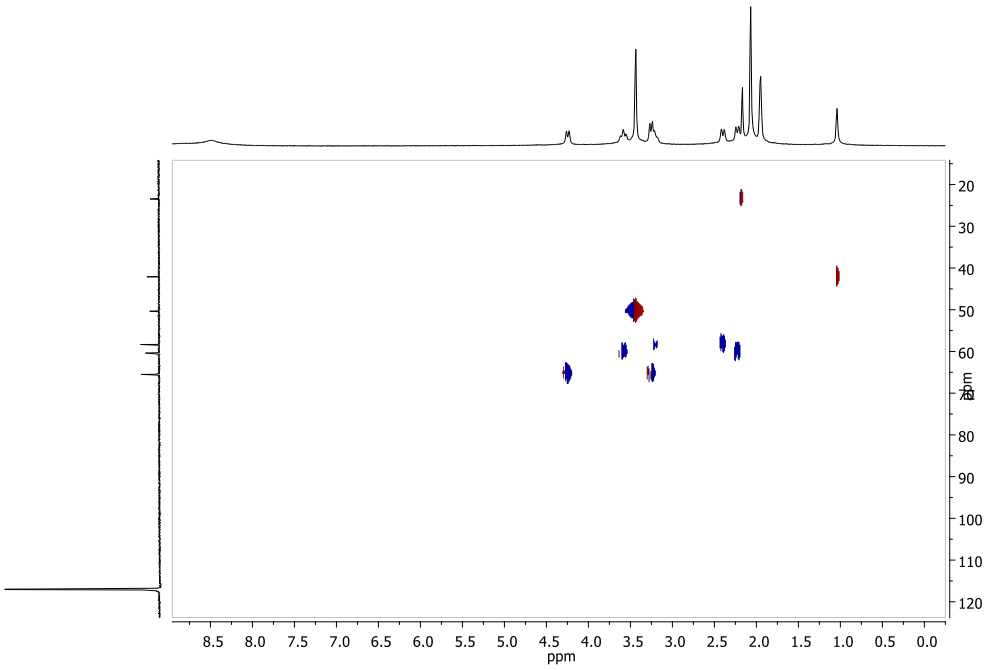

Figure S25. HMBC spectrum of [**Pd-1c**·$(AcO)_2$]$(CF_3SO_3)_2$ molecular clip (isolated major conformer), (CD_3CN, 328 K, 400 MHz).

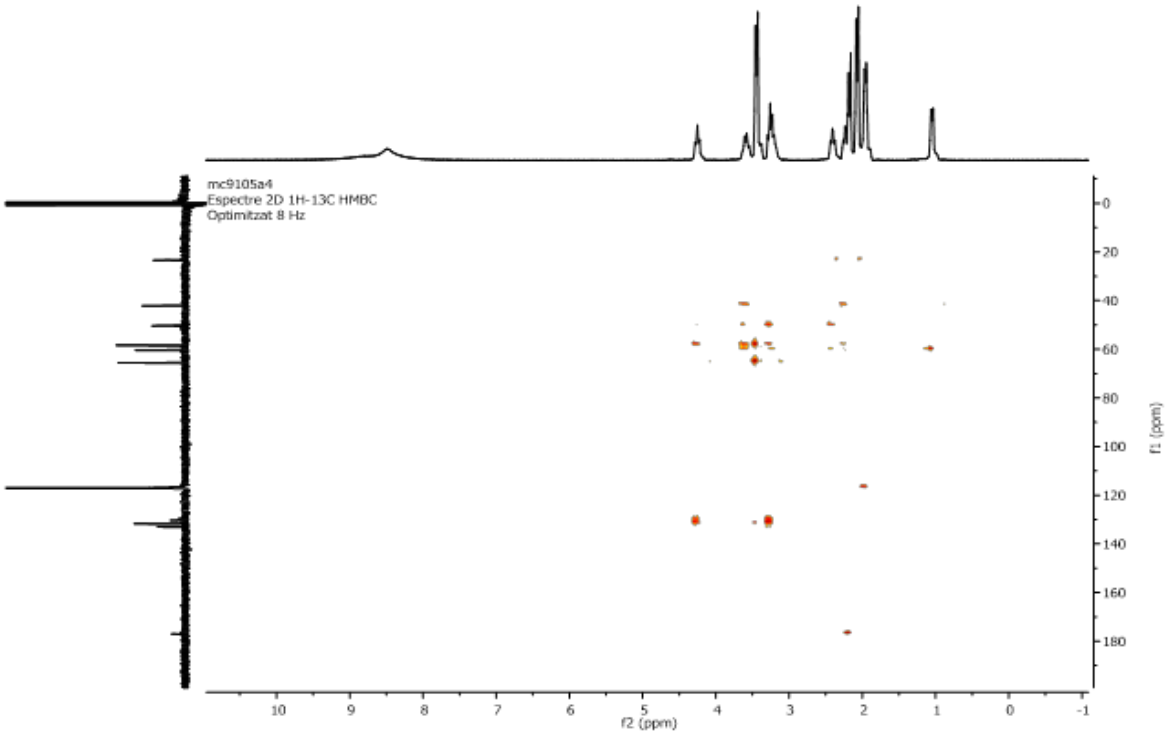

Figure S26. HRMS spectra of [**Pd-1c**·$(AcO)_2$]$(CF_3SO_3)_2$ molecular clip. Experimental conditions: 100 µM in CH_3CN, registered with a Bruker MicroTOF-Q-II exact mass spectrometer.

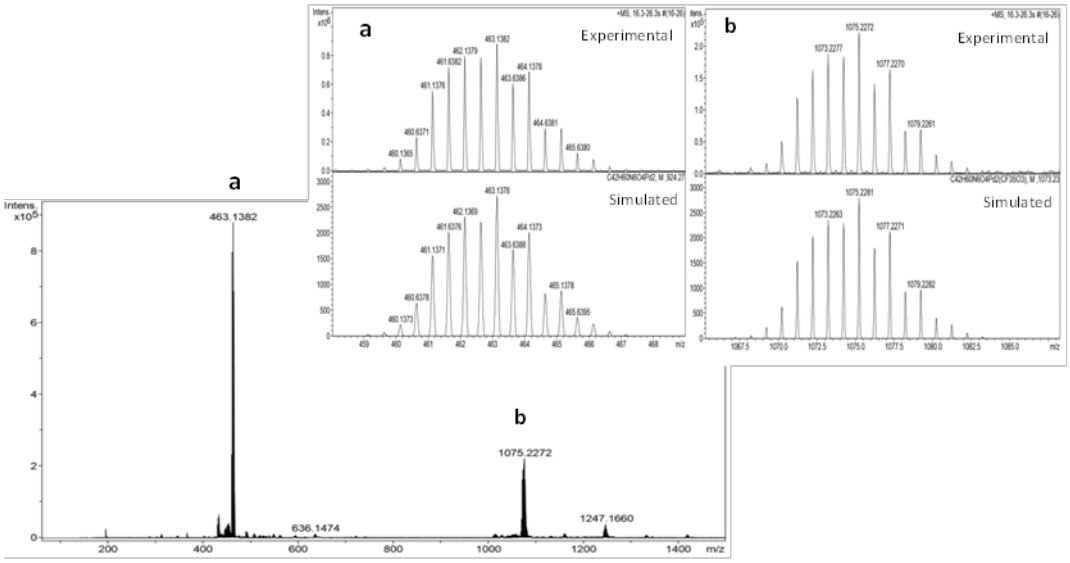

Figure S27. Crystal structure of macrocyclic compound **Pd-1c**·$(AcO)_4$. Pd (II) presents a d^8 electronic configuration which enforce palladium ions to adopt a tetra-coordinated square-planar geometry formed by three N atoms of the macrocyclic ligand **1c** and one O atom from the carboxylate group, which coordinates in a mono-dentate mode.

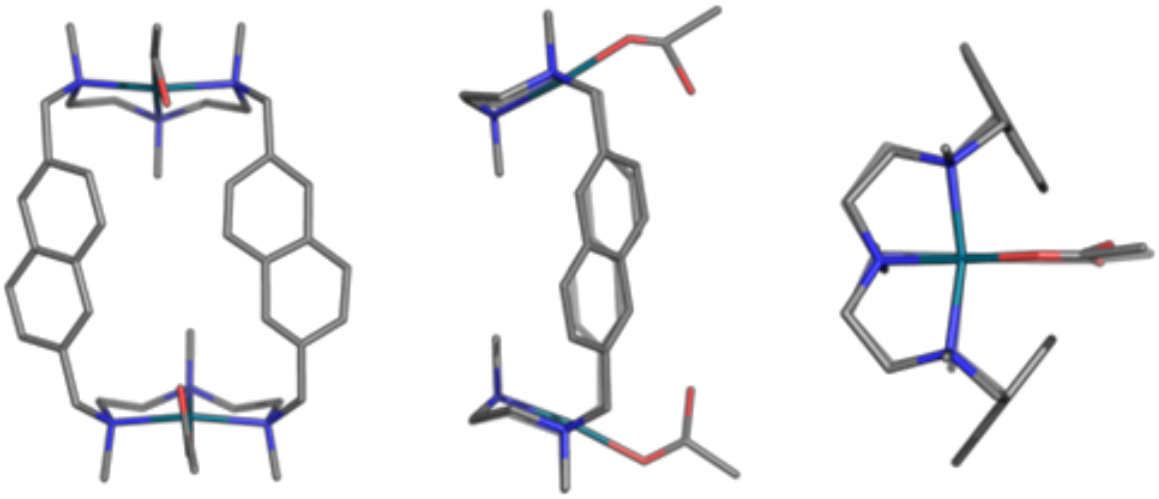

Figure S28. HRMS spectrum of **5**·$(CF_3SO_3)_8$ nanocapsule. Inset: selected obtained (top) and simulated peaks in blue (bottom). Experimental conditions: 100 µM CH_3CN, registered with a Bruker MicroTOF-Q-II exact mass spectrometer.

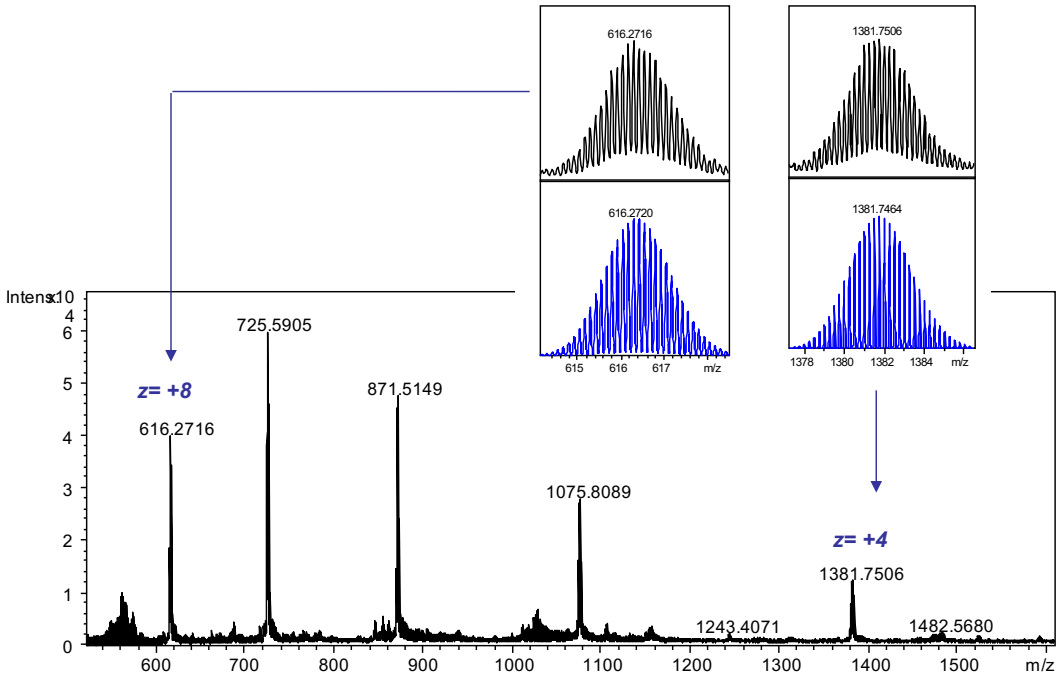

Figure S29. HRMS spectrum of **5**·$(BArF)_8$ nanocapsule. Inset: selected obtained (top) and simulated peaks in blue (bottom). Experimental conditions: 100 µM CH_3CN, registered with a Bruker MicroTOF-Q-II exact mass spectrometer.

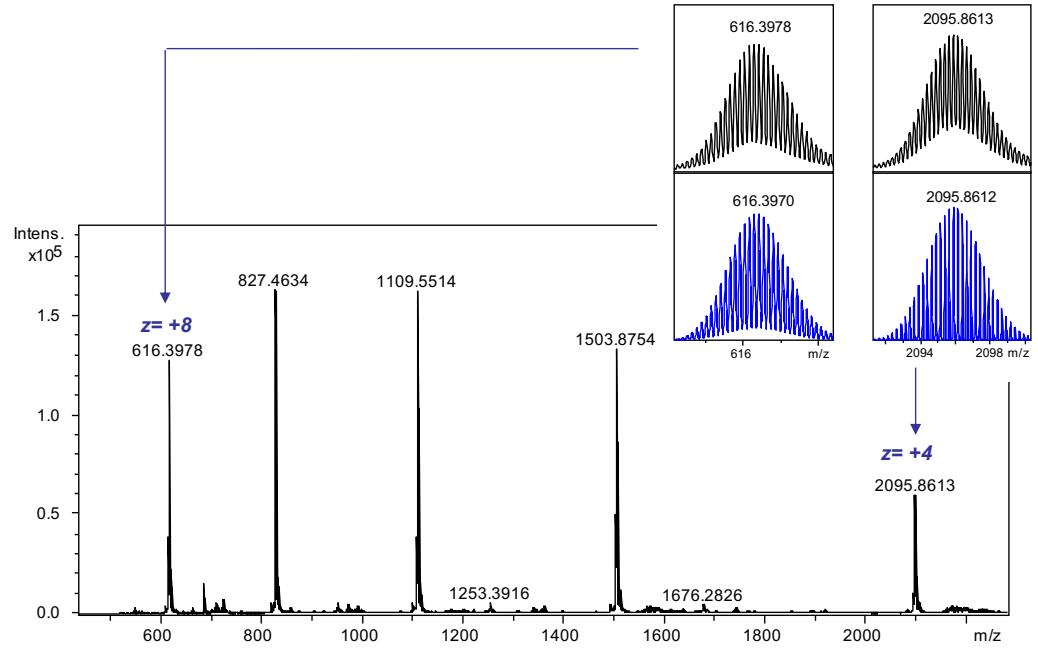

Figure S30. ^{1}H-NMR spectrum of **5**·$(BArF)_8$ molecular capsule**.** Experiment performed in CD_3CN at 328 K (400 MHz), (* = internal standard: mesitylene).

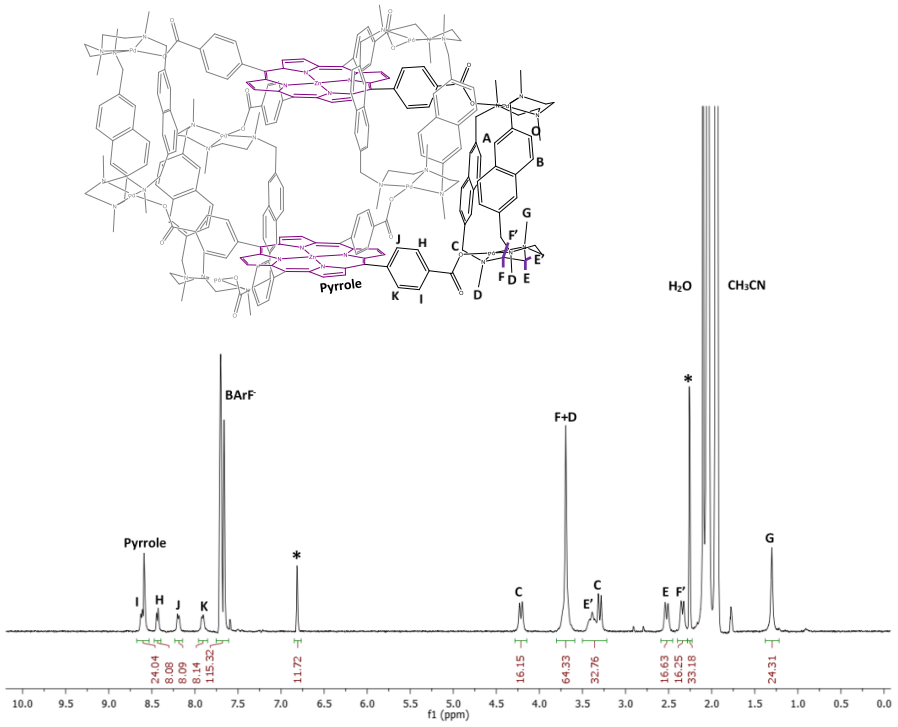

Figure S31. ^{1}H-NMR spectra of **5**·$(BArF)_8$ nanocapsule at different temperatures showing broad bands at 8.5-9.5 ppm corresponding to A and B naphthalene protons, see Figure S32 (CD_3CN, 400 MHz).

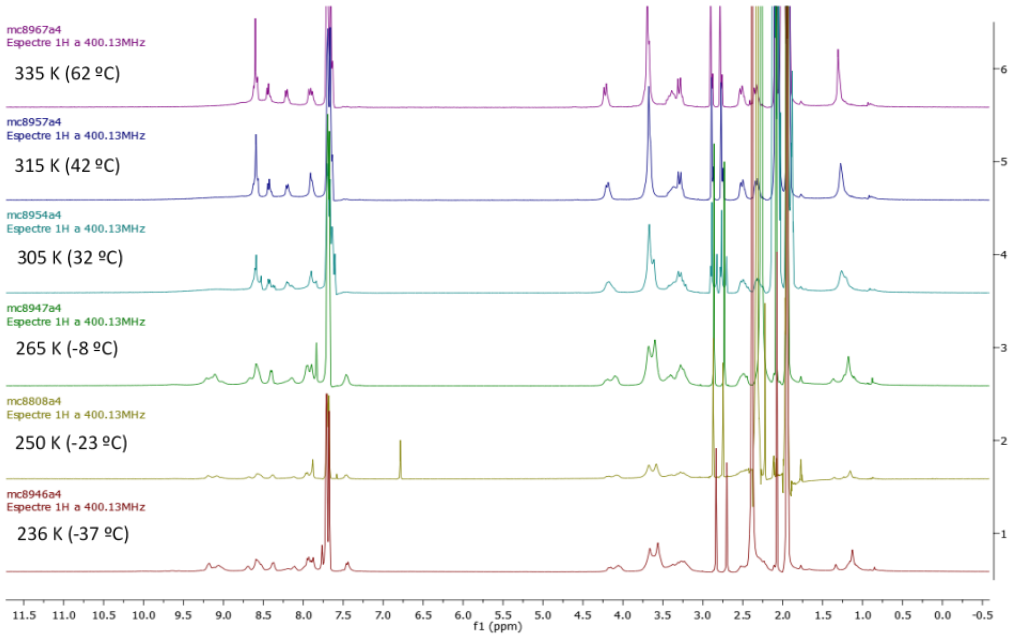

Figure S32. COSY-NMR spectrum of **5**·$(BArF)_8$ molecular capsule (CD_3CN, 328 K, 400 MHz).

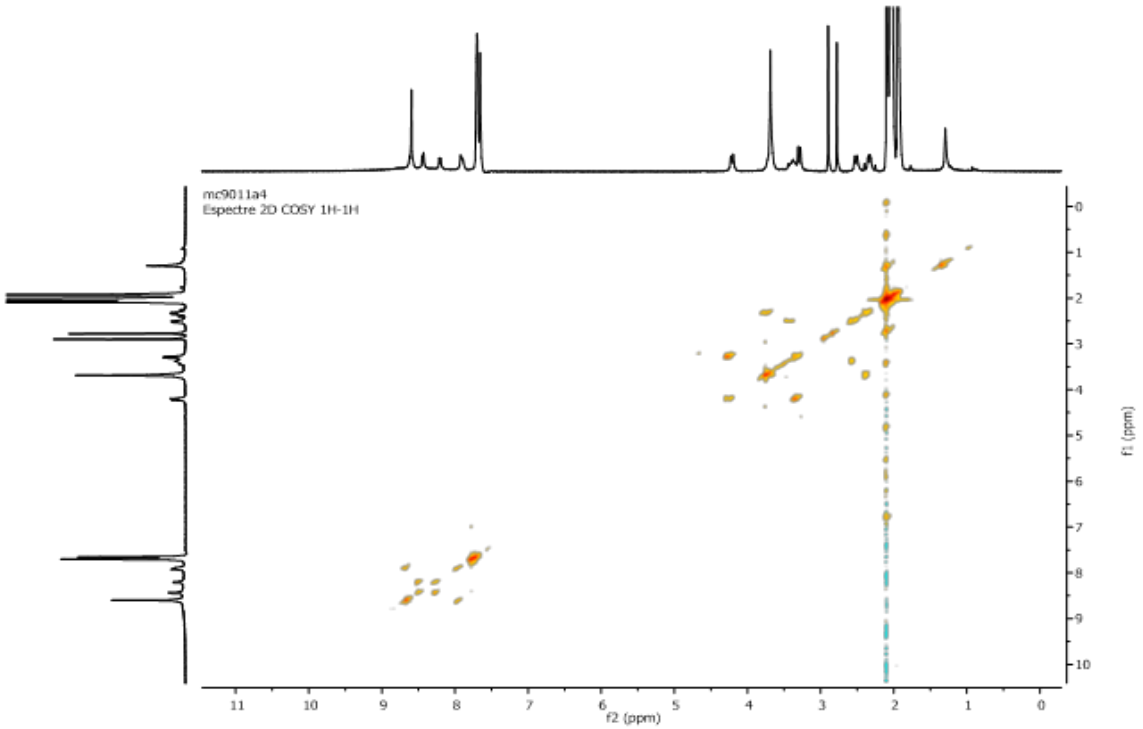

Figure S33. NOESY-NMR spectrum of **5**·$(BArF)_8$ molecular capsule (CD_3CN, 328 K, 400 MHz).

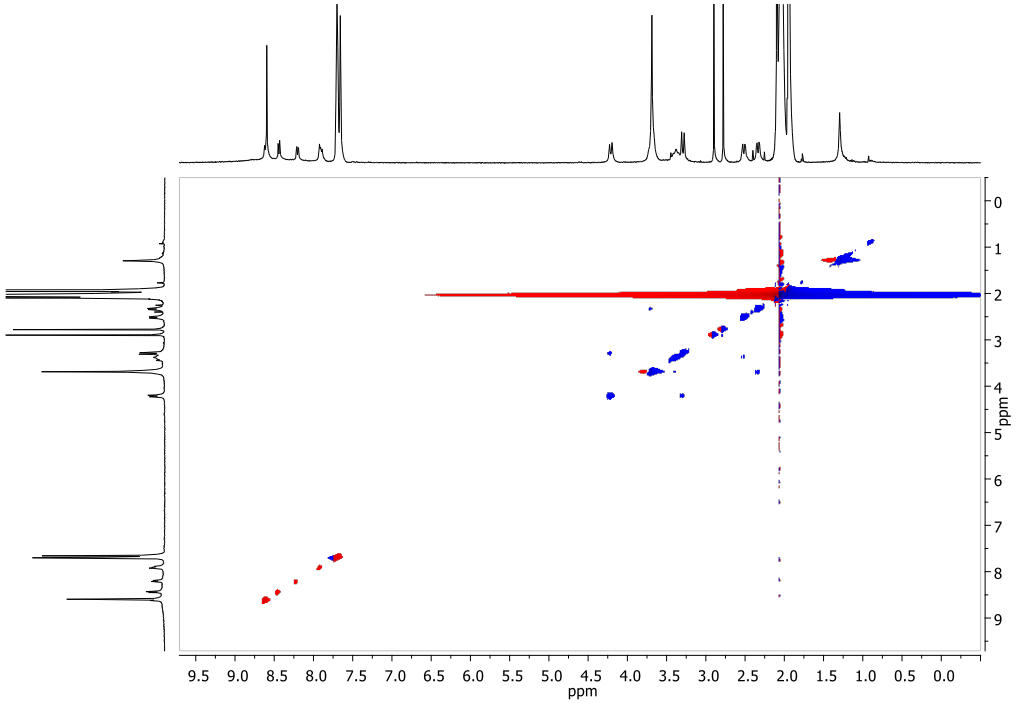

Figure S34. ^{13}C-NMR spectrum of **5**·$(BArF)_8$ molecular capsule (CD_3CN, 328 K, 400 MHz).

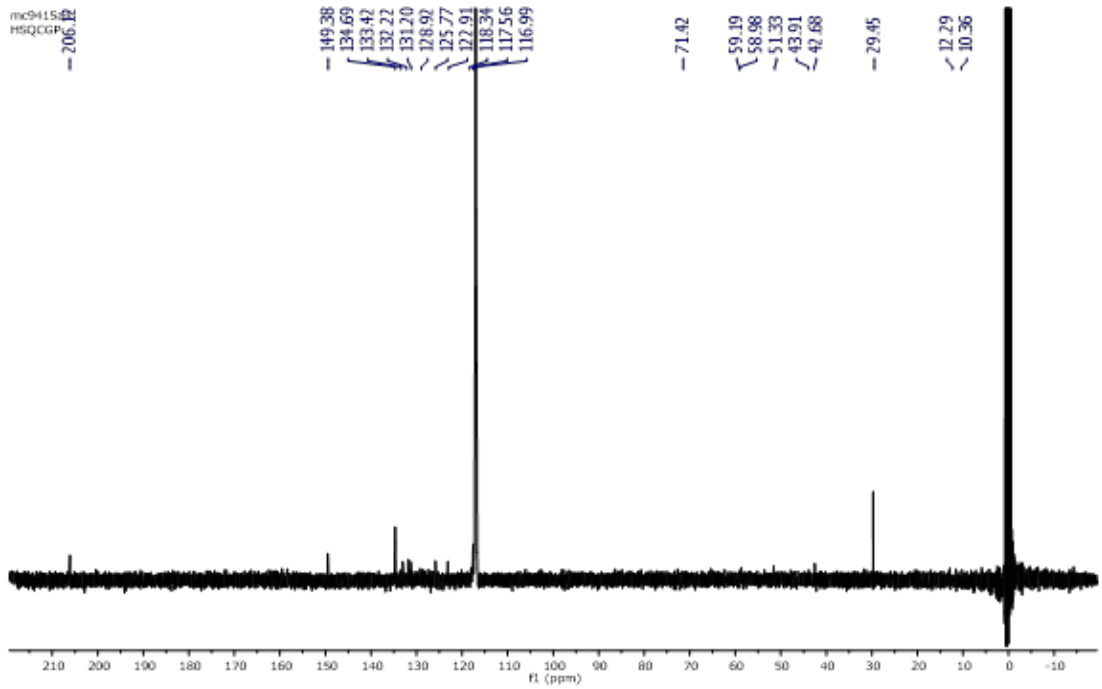

Figure S35. HSQCed-NMR spectrum of **5**·$(BArF)_8$ molecular capsule (CD_3CN, 328 K, 400 MHz).

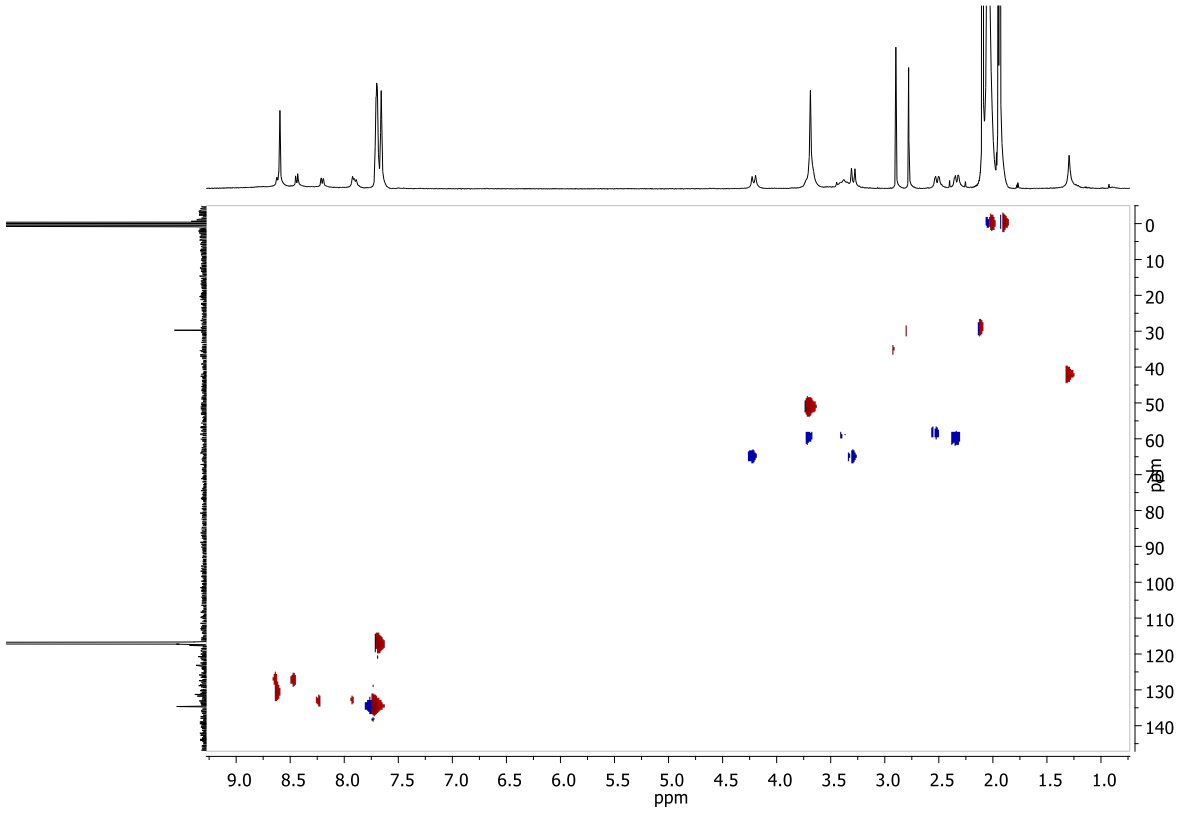

Figure S36. HMBC-NMR spectrum of **5**·$(BArF)_8$ molecular capsule (CD_3CN, 328 K, 400 MHz).

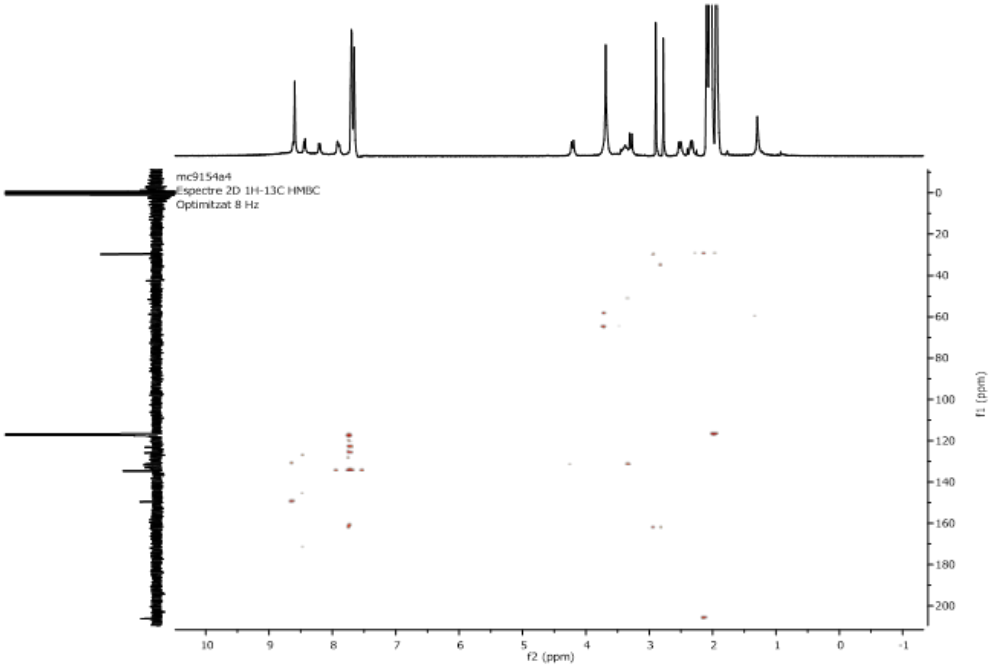

Figure S37. DOSY NMR spectrum of nanocage **5**·$(BArF)_8$. Affording a diffusion coefficient (D) of $D=10^{-9.506}$ m^2 s^{-1} ($D_{CD3CN}= 10^{-8.419}$ m^2 s^{-1}) at 298 K.

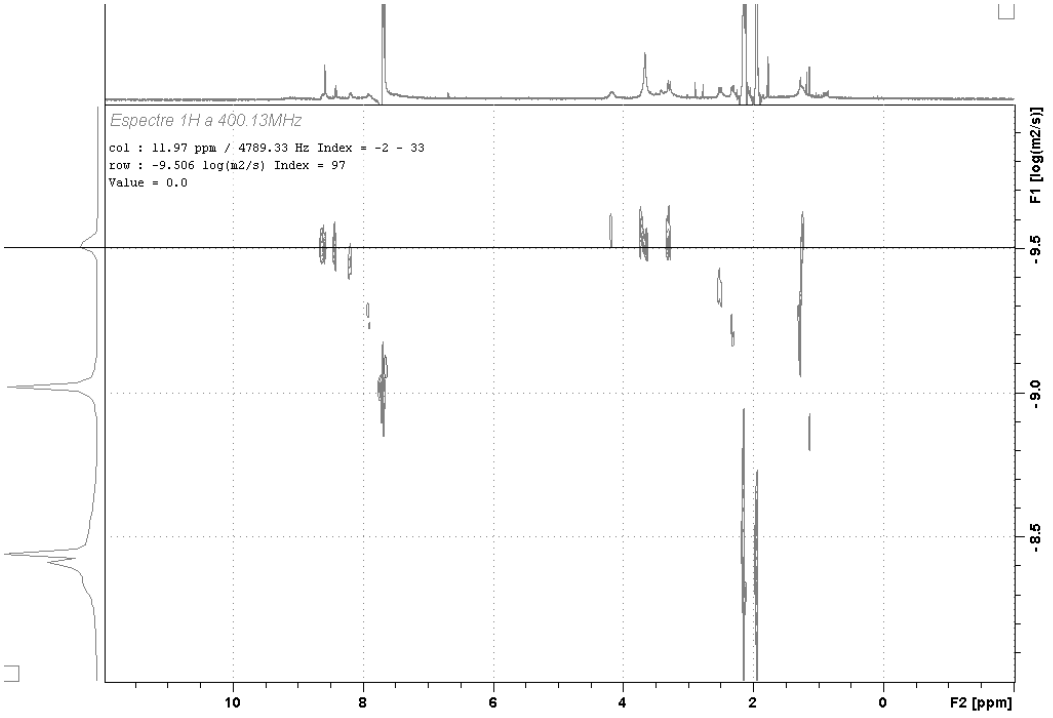

Figure S38. a) X-Ray diffraction of the **5**·$(CF_3SO_3)_8$ naphthalene nanocapsule (front and top views, M···M distances shown). Counter ions and hydrogens have been omitted for clarity (Grey: C, red: O, blue: N, green: Pd). **b**) Hydrodynamic ratio (r_H) of $\mathbf{5}^{8+}$ capsule calculated from the diffusion coefficients (D) extracted from the DOSY NMR experiments in CD_3CN and from the X-ray structure. **c**) Calculated volumes of the spheres that can occupy the inner void space (using Platon).

a)

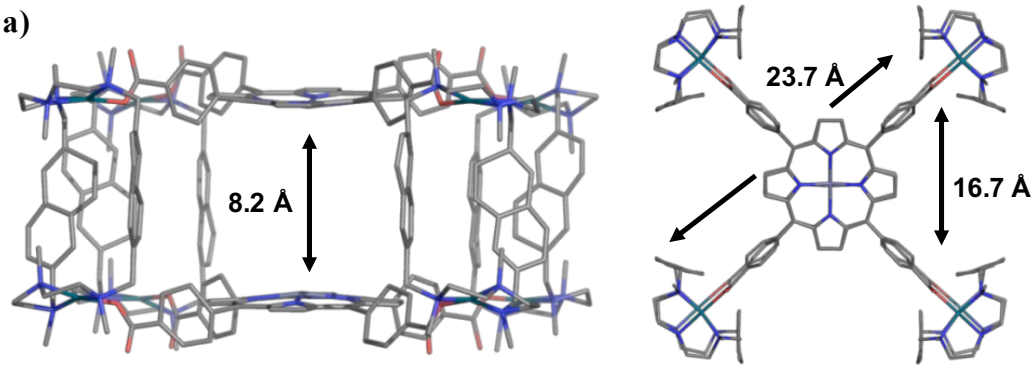

b)

	D (m^2s^{-1})	r_H (Å)	XRD radii (Å)
$\mathbf{5}^{8+}$	$3.1 \cdot 10^{-10}$	18.5	17.2

c)

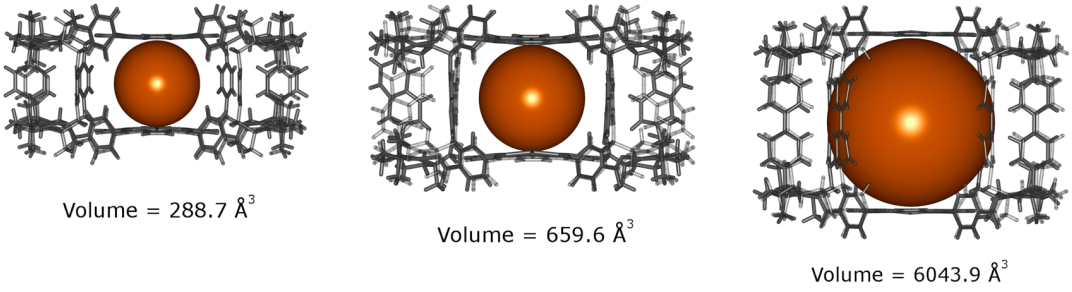

Figure S39. HRMS spectrum of $C_{60}\subset$**5**·$(BArF)_8$ host-guest complex, formed after mixing a solution of **5**·$(BArF)_8$ in acetonitrile and C_{60} dissolved in toluene, in a 1:1 molar ration (v/v-MeCN/TL, 4/1**)**. Experimental conditions: 100 µM in CH_3CN, registered with a Bruker MicroTOF-Q-II exact mass spectrometer.

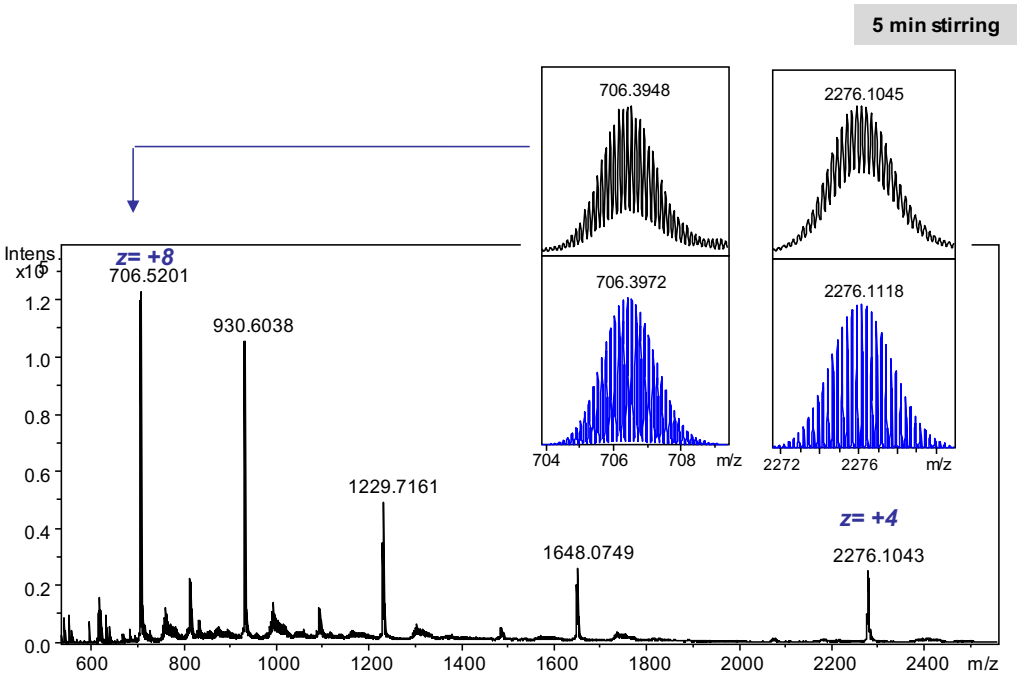

Figure S40. UV-Vis monitoring of the titration of **5**·$(BArF)_8$ nanocapsule with fullerene C_{60}. Fixed total concentration ($6.46\cdot10^{-6}$ M) of nanocapsule in Toluene/Acetonitrile (9/1).

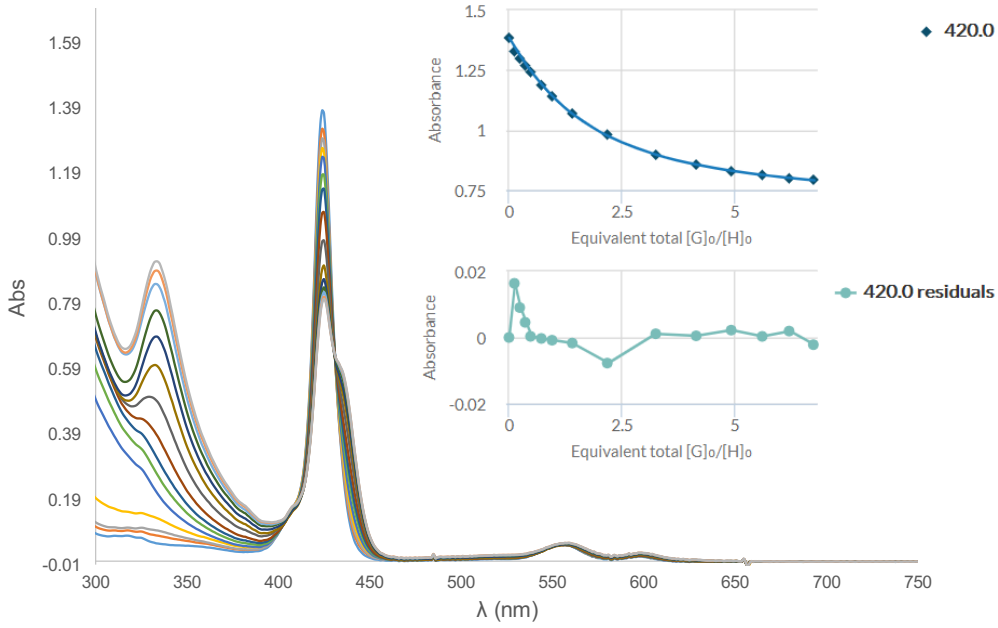

Figure S41. ^{1}H-NMR spectrum of $C_{60}\subset$4·$(BArF)_8$ adduct. Experiment performed in CD_3CN at 328 K (400 MHz).

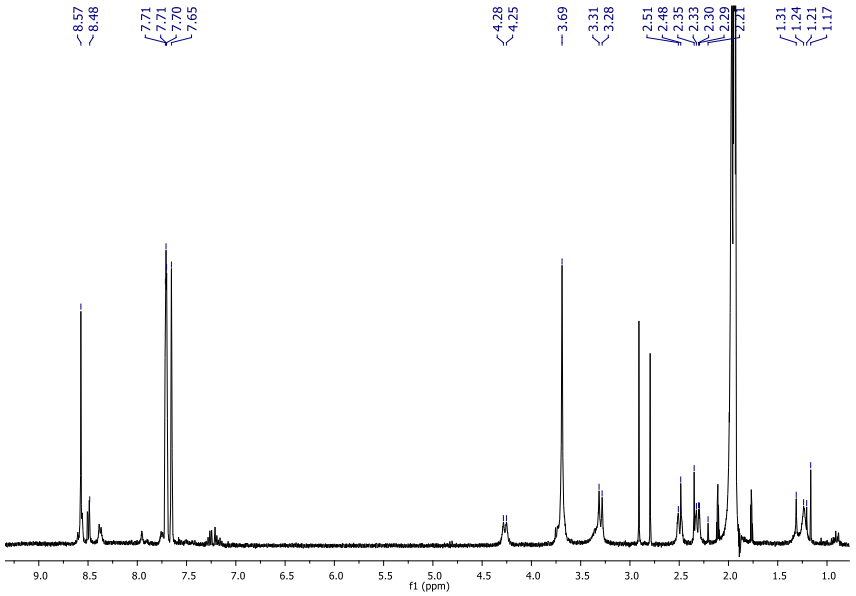

Figure S42. HRMS spectrum of $C_{70}\subset$**5**·$(BArF)_8$ host-guest complex, formed after mixing a solution of **5**·$(BArF)_8$ in acetonitrile and C_{70} dissolved in toluene, in a 1:2 molar ration (v/v-MeCN/TL, 4/1**)**. Experimental conditions: 100 µM in CH_3CN, registered with a Bruker MicroTOF-Q-II exact mass spectrometer.

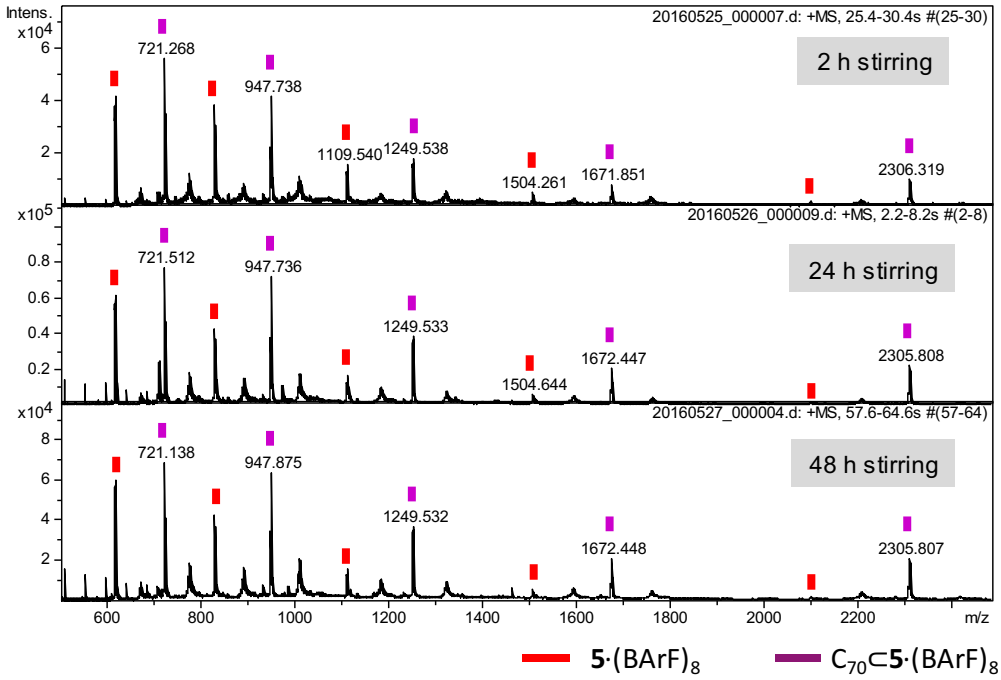

Figure S43. UV-Vis monitoring of the titration of **5**·$(BArF)_8$ nanocapsule with fullerene C_{70}. Fixed total concentration ($6.46 \cdot 10^{-6}$ M) of nanocapsule in Toluene/Acetonitrile (9/1).

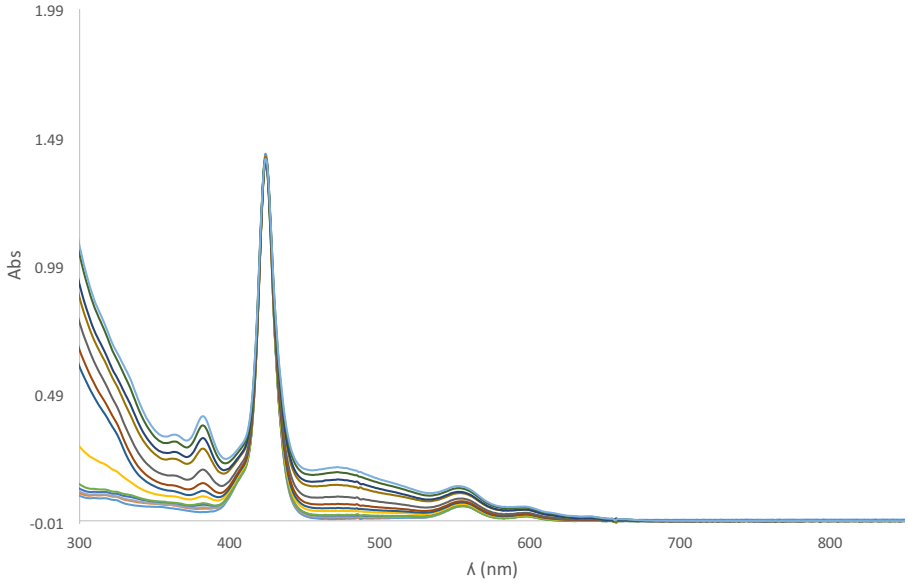

Figure S44. Zn···Zn distance and N(5)-Zn(5)-C(ful)-C(ful) dihedral angle measured over the 500ns of MD trajectory for C_{60} and C_{70} encapsulated inside **5**$(Cl)_8$.

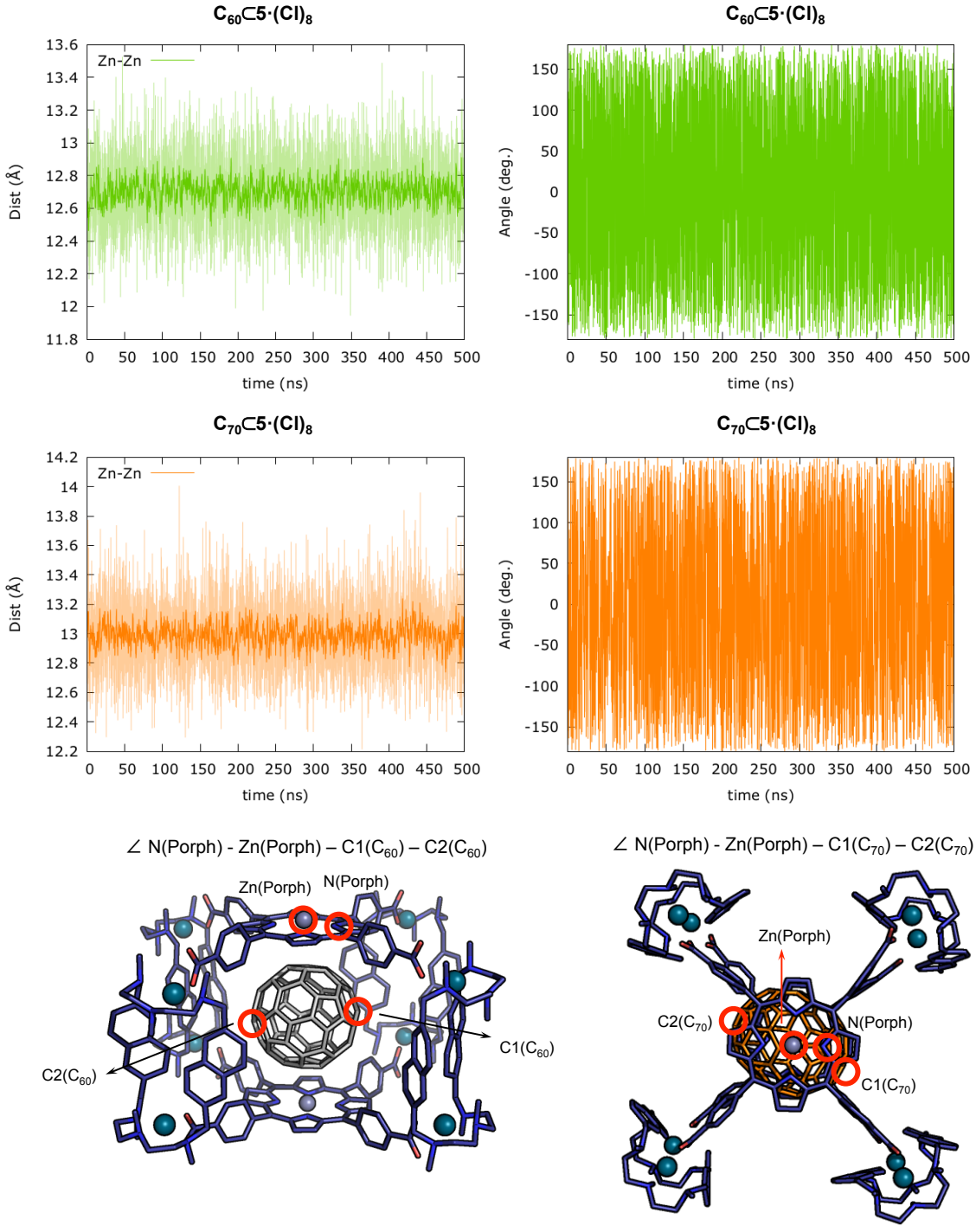

The large fluctuation of the defined dihedral angles indicates that encapsulated C_{60} and C_{70} can adopt many different orientations inside the supramolecular cage **5**.

Figure S45. HRMS spectra following over time the formation of the $C_{60}\subset$**5**$\cdot(CF_3SO_3)_8$ host-guest complex, formed after soaking **5**$\cdot(CF_3SO_3)_8$ capsule in the **solid state** C_{60} dissolved in toluene, in a 1:8 molar ration. Experimental conditions: 100 µM in CH_3CN, registered with a Bruker MicroTOF-Q-II exact mass spectrometer.

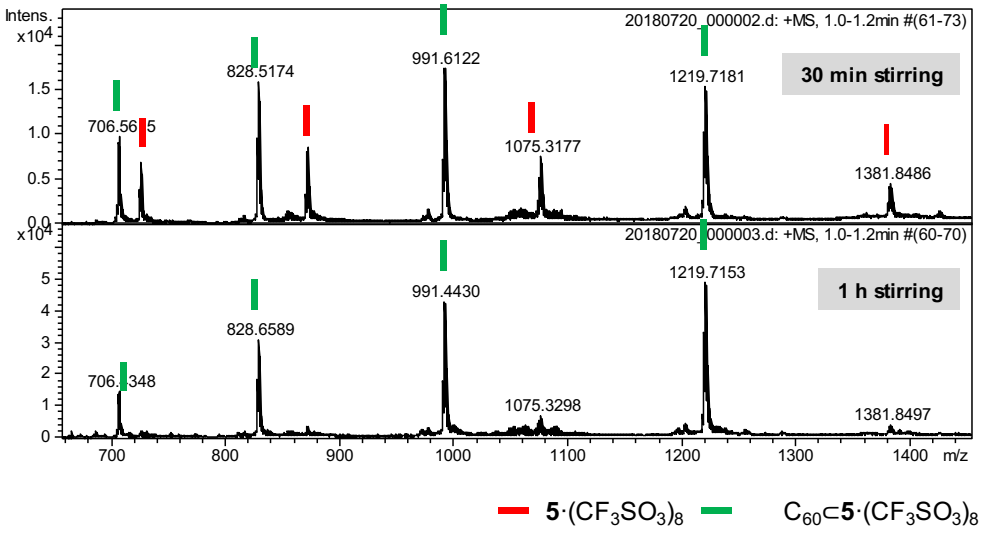

Figure S46. HRMS spectra following over time the formation of fullerene extract-**5**$\cdot(BArF)_8$ host-guest complexes. Capsule/extract ratio (molar): 1/2. Experiment performed with the capsule in acetonitrile solution and the fullerenes in toluene solution. Experimental conditions: 100 µM in Toluene/CH_3CN (4/1), registered with a Bruker MicroTOF-Q-II exact mass spectrometer.

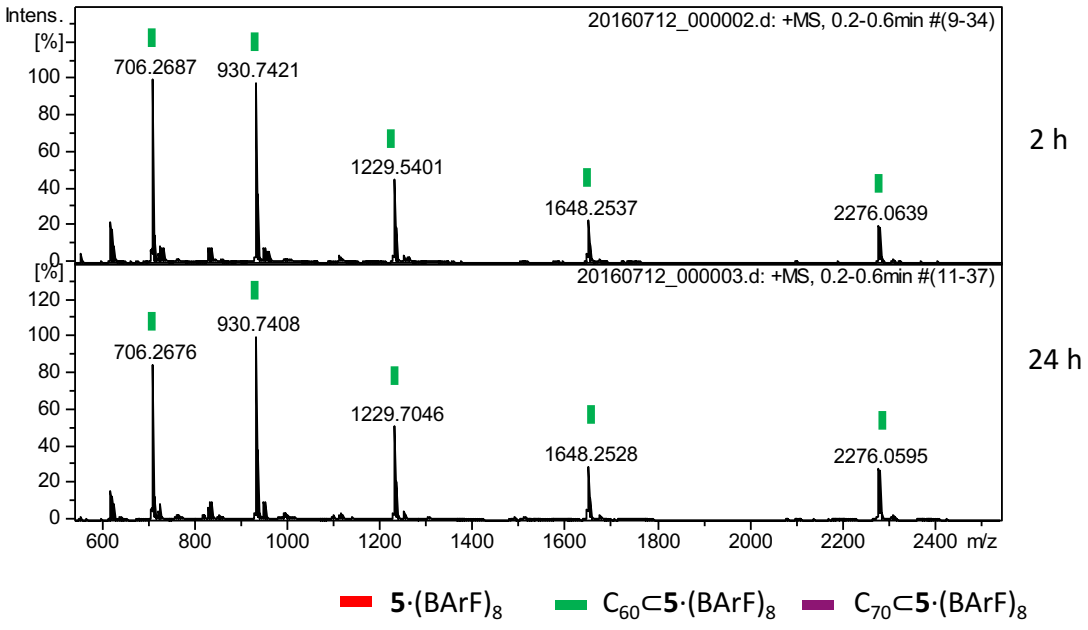

Figure S47. HRMS spectra following over time the formation of fullerene extract-**5**·$(CF_3SO_3)_8$ host-guest complexes. Capsule/extract ratio (molar ratio considering all extract as C_{60}): 1/8. Experiment performed with the **capsule in solid** and the fullerenes in toluene solution. Experimental conditions: 100 µM in Toluene/CH_3CN (4/1), registered with a Bruker MicroTOF-Q-II exact mass spectrometer.

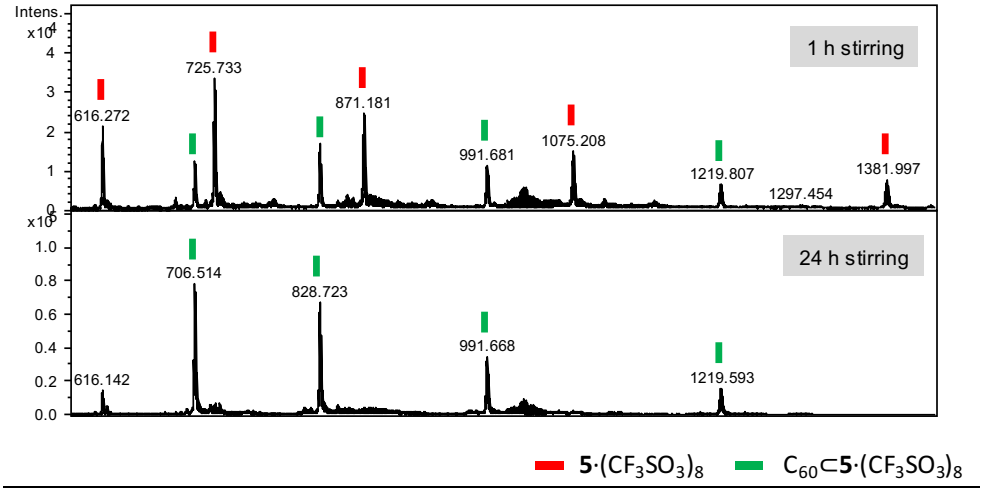

Figure S48. HRMS spectrum of [N-methylpyrrolidine-C_{60}]⊂**5**·$(BArF)_8$ host-guest complex, formed after mixing a solution of **5**·$(BArF)_8$ in acetonitrile and C_{60}-fulleropyrrolidine dissolved in toluene, in a 1:1 molar ration (v/v-MeCN/TL, 4/1). Experimental conditions: 100 µM in CH_3CN, registered with a Bruker MicroTOF-Q-II exact mass spectrometer.

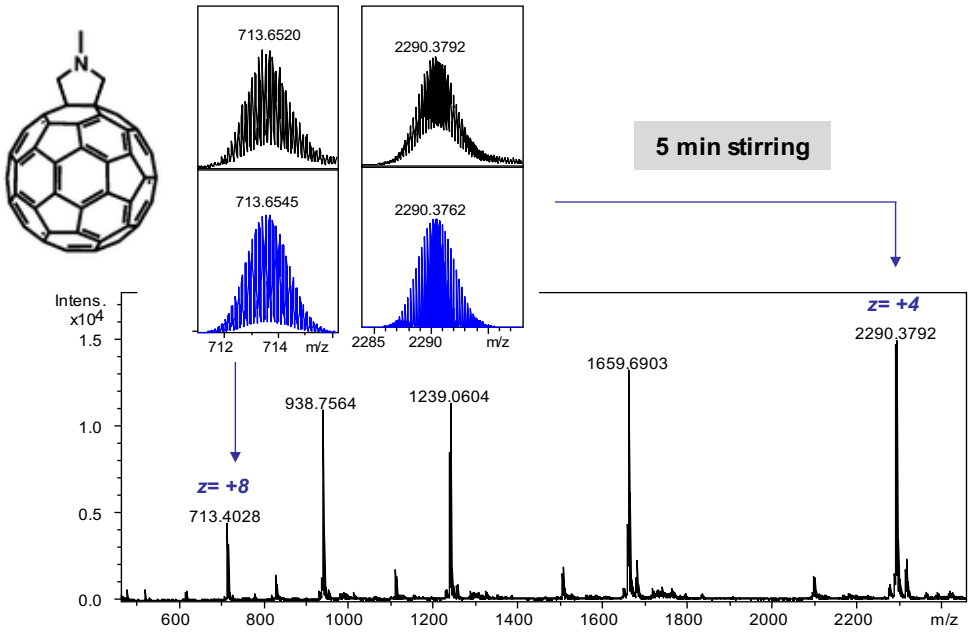

Figure S49. HRMS spectrum of [PCBM-C_{60}]⊂**5**·$(BArF)_8$ host-guest complex, formed after mixing a solution of **5**·$(BArF)_8$ in acetonitrile and PCBM-C_{60} dissolved in toluene, in a 1:1 molar ration (v/v-MeCN/TL, 4/1). Experimental conditions: 100 µM in CH_3CN, registered with a Bruker MicroTOF-Q-II exact mass spectrometer.

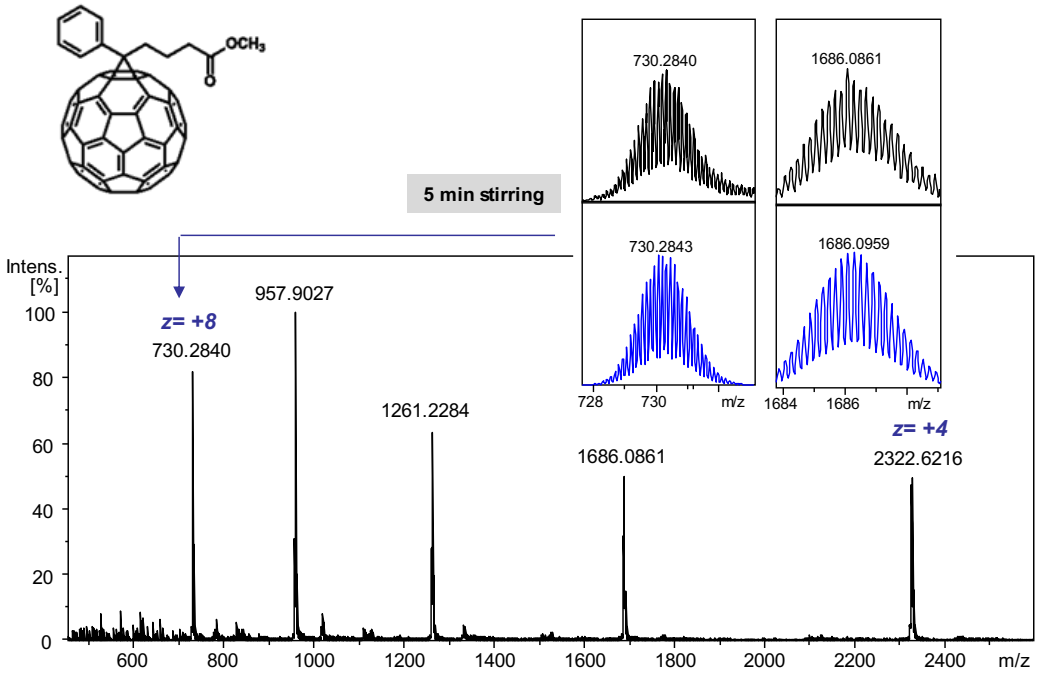

Figure S50. UV-Vis monitoring of the titration of **5**·$(BArF)_8$ nanocapsule with N-methylpyrrolidine-C_{60}. Fixed total concentration ($6.46 \cdot 10^{-6}$ M) of nanocapsule in Toluene/Acetonitrile. (9/1).

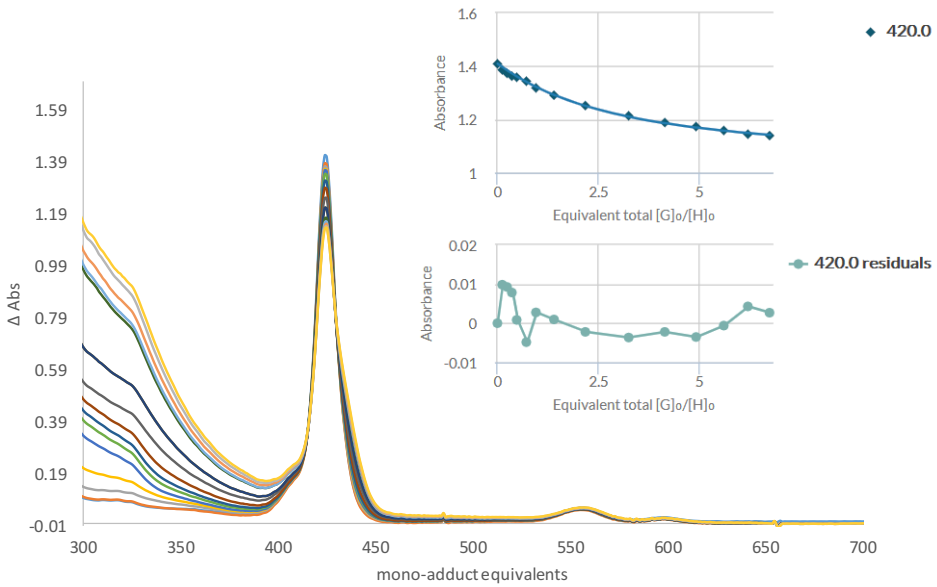

Figure S51. UV-Vis monitoring of the titration of **5**·$(BArF)_8$ nanocapsule with fullerene PCBM-C_{60} adduct. Fixed total concentration ($6.46 \cdot 10^{-6}$ M) of nanocapsule in Toluene/Acetonitrile. (9/1).

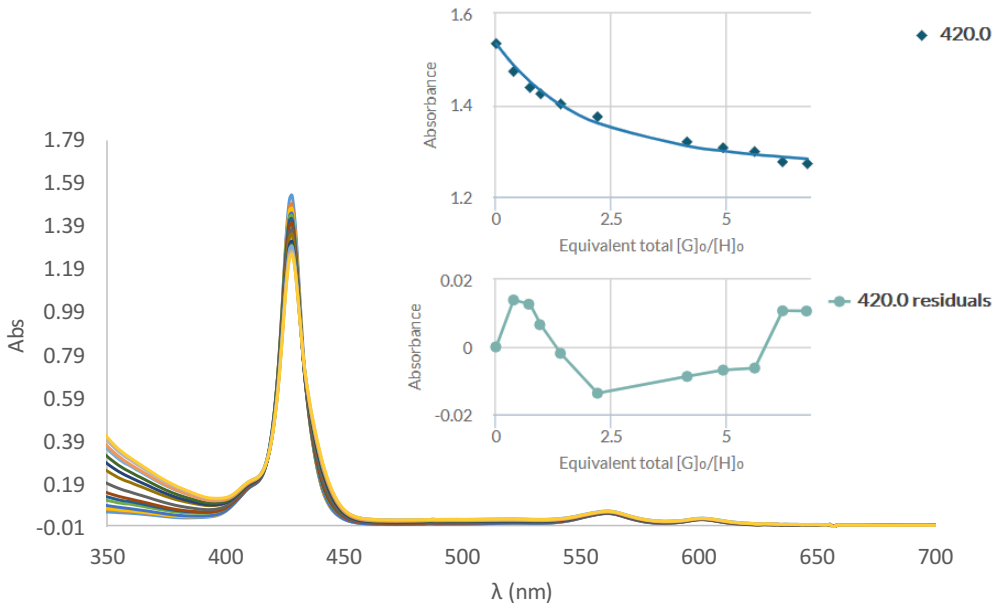

Figure S52. HRMS spectra following over time the formation of [N-methylpyrrolidine-C_{60}]⊂**5**·$(CF_3SO_3)_8$ host-guest complex, formed after soaking **5**·$(CF_3SO_3)_8$ capsule in the **solid state** C_{60} dissolved in toluene, in a 1:8 molar ration. Experimental conditions: 100 µM in CH_3CN, registered with a Bruker MicroTOF-Q-II exact mass spectrometer.

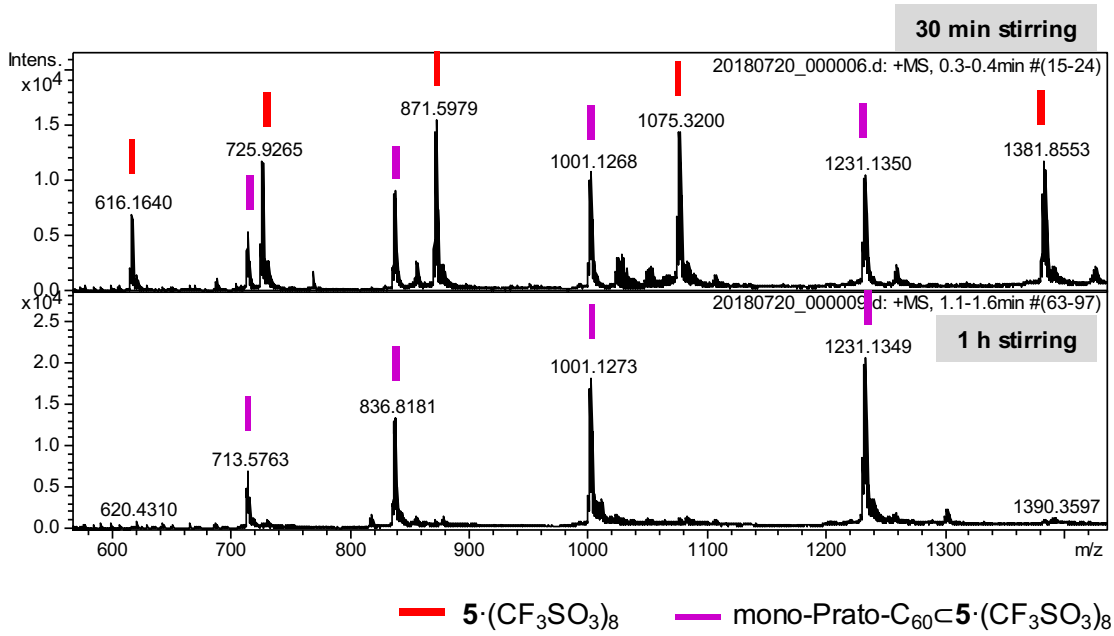

Figure S53. HRMS spectra following over time the formation of the PCBM-C_{60}⊂**5**·$(CF_3SO_3)_8$ host-guest complex, formed after soaking **5**·$(CF_3SO_3)_8$ capsule in the **solid state** C_{60} dissolved in toluene, in a 1:8 molar ration. Experimental conditions: 100 µM in CH_3CN, registered with a Bruker MicroTOF-Q-II exact mass spectrometer.

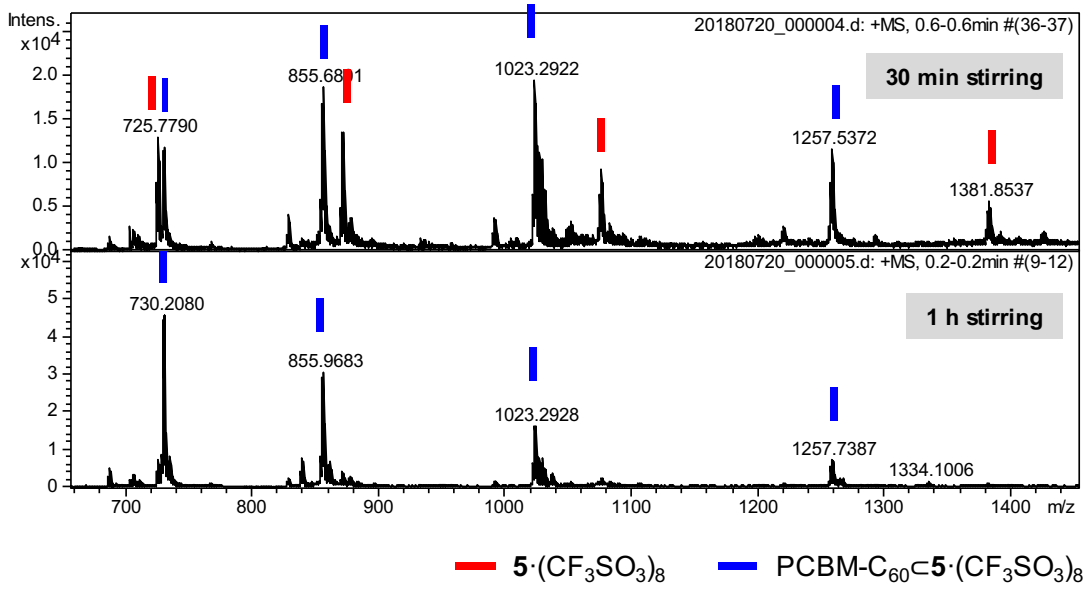

Figure S54. HRMS spectrum of the mixture of 1 eq. of 5·(BArF)8 with 2.5 eq. of C60 and 2.5 eq. of PCBM-C60. Reaction time 2.5 h in TL/MeCN (4/1). Experimental conditions: 100 µM in Toluene/CH3CN (4/1), registered with a Bruker MicroTOF-Q-II exact mass spectrometer.

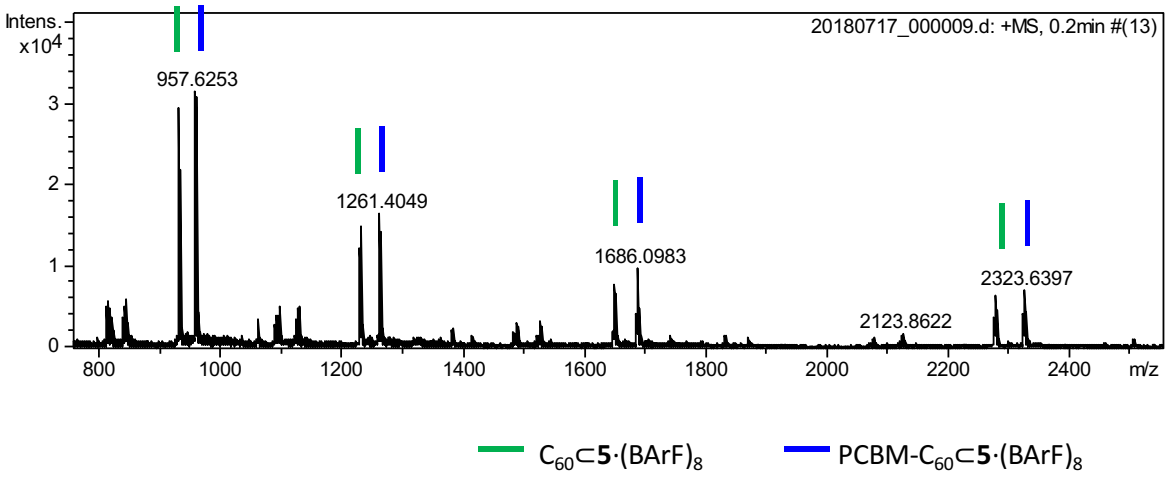

Figure S55. HRMS spectrum of the mixture of 1 eq. of **5**·$(BArF)_8$ with 2.5 eq. of C_{60} and 2.5 eq. of N-methylpyrrolidine-C_{60}. Reaction time 2.5 h in TL/MeCN (4/1). Experimental conditions: 100 µM in Toluene/CH_3CN (4/1), registered with a Bruker MicroTOF-Q-II exact mass spectrometer.

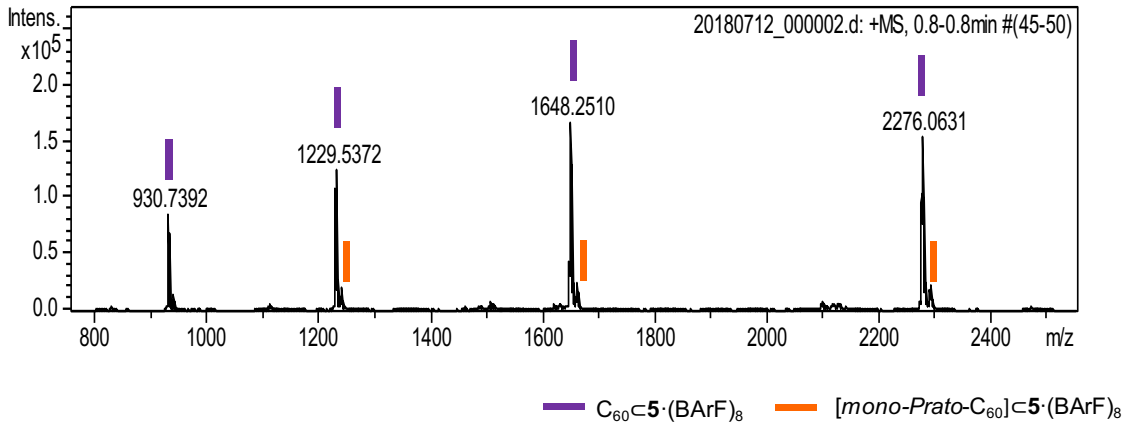

Figure S56. HRMS spectrum of the mixture of **5**·$(BArF)_8$ with 0.25 eq. of C_{60} and 0.25 eq. of (mono)-*n*-pyrrolidine-C_{60}**.** Experimental conditions: 100 µM in Toluene/CH_3CN (4/1), registered with a Bruker MicroTOF-Q-II exact mass spectrometer. substoichiometric additions of C_{60} and N-methylpyrrolidine-C_{60} to **5**·$(BArF)_8$ confirmed the same ionization behavior of C_{60}-host and [N-methylpyrrolidine-C_{60}]-host, meaning that the relative intensity of the peaks corresponding to C_{60}-host and adduct-host with the same charge reproduce their relative concentration in solution.

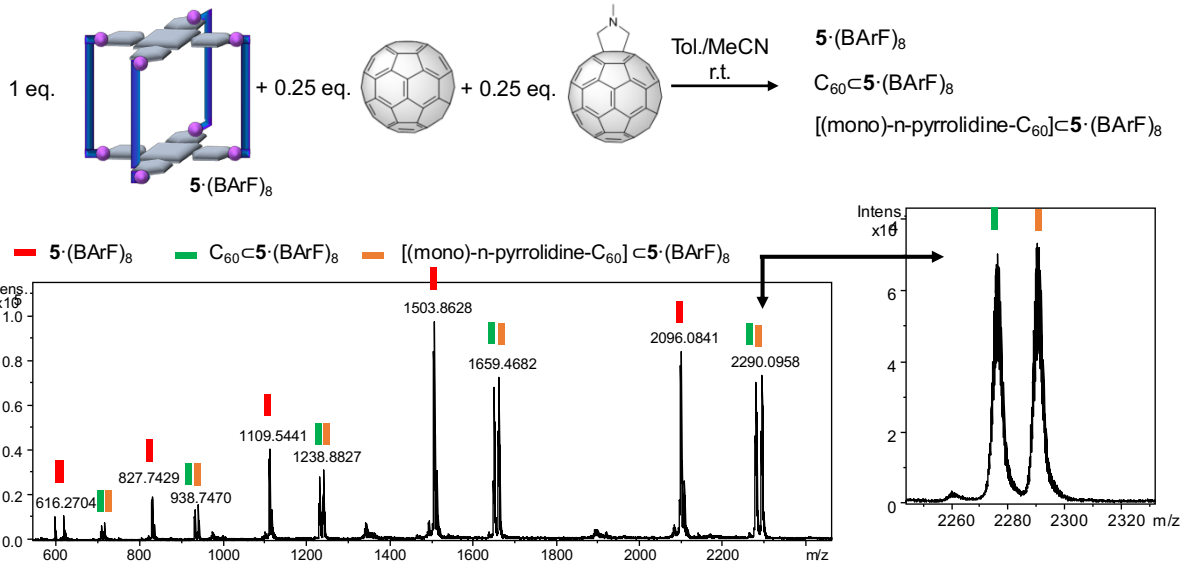

Figure S57. HRMS spectrum of the mixture of **a)** 1 eq. of 5·(BArF)8 with 0.9 eq. of C60 and 0.9 eq. of N-methylpyrrolidine-C_{60} (reaction time 1.5 h in TL/MeCN (4/1)) and **b)** capsule after applying the solvent-washing protocol (20 ml of CS_2). Experimental conditions: 100 µM in Toluene/CH3CN (4/1), registered with a Bruker MicroTOF-Q-II exact mass spectrometer.

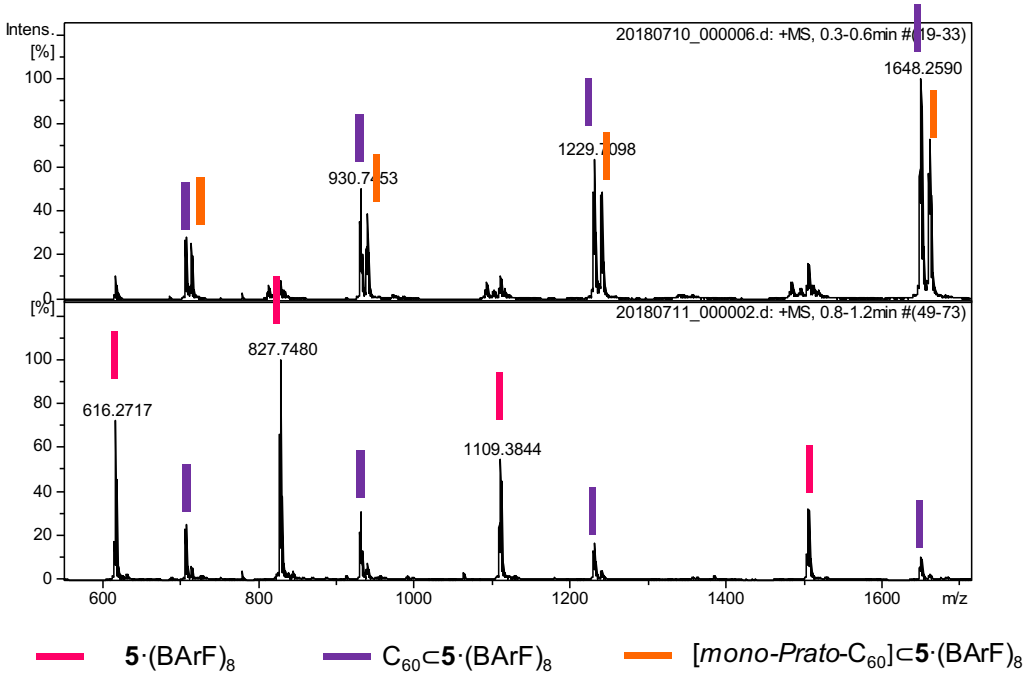

3. Supplementary Tables

Table S1. Crystal Data and Structure Refinement for **Pd-1c**·$(CH_3COO)_4$ and **5**·$(CF_3SO_3)_8$.

	Pd-1c·$(CH_3COO)_4$	**5**·$(CF_3SO_3)_8$
Formula	$C_{48}\,H_{69}\,N_7\,O_8\,Pd_2$, $2(C_2\,H_3\,O_2)$	$C_{248}\,N_{32}\,O_{16}\,Pd_8\,Zn_2$
CDD code	**1561152**	**1561153**
fw	1084.90	4930.91
cryst system	Monoclinic	Orthorhombic
space group	C 2/c	P m c b
a (Å)	38.293(6)	26.400(6)
b (Å)	9.5059(14)	27.470(6)
c (Å)	34.347(6)	27.690(6)
α (deg)	90.00	90.00
β (deg)	117.823(2)	90.00
γ (deg)	90.00	90.00
V (Å^3)	11057(3)	20081
Z	8	2
*D*c (Mg cm-3)	1.303	0.815
T (K)	130(2) K	100(2)
λ (Mo KR) (Å)	0.71073	0.69873
μ (mm-1)	0.703	0.506
2*Θ* max (deg)	28.39	23.62
reflns collected	33088	49214
independent reflns	12753 (*R*int= 0.0818)	13031 0.0782
parameters	527	658
GOF on F^2	0.967	0.857
R/R_w	R1 = 0.0929, wR2 = 0.2415	R1 = 0.1142, wR2 = 0.3019

4. Supplementary Videos

Supplementary videos can be downloaded from the link provided in the online version of the article.

Supplementary Video VS1. MD trajectory for the empty **5**·$(Cl)_8$.
Front view: Video_S1a.mpg
Top view: Video_S1b.mpg

Supplementary Video VS2. MD trajectory for the C_{60}⊂**5**·$(Cl)_8$ host-guest complex.
Front view: Video_S2a.mpg
Top view: Video_S2b.mpg
Front view, stick model: Video_S2c.mpg

Supplementary Video VS3. MD trajectory for the C_{70}⊂**5**·$(Cl)_8$ host-guest complex.
Front view: Video_S3a.mpg
Top view: Video_S3b.mpg

5. Supplementary References

(1) Gao-Yi Xie, Long Jiang, and Tong-Bu Lu. Dalton Transactions. 2013, 42, 14092-14099.
(2) Ribas, X., Dias, J. C., Morgado, J., Wurst, K., Almeida, M., Parella, T., Veciana, J., and Rovira, C. *Angew. Chem. Int. Ed.* **2004**, 43, 4049-4052.
(3) R. Salomon-Ferrer, A. W. Götz, D. Poole, S. Le Grand and R. C. Walker, *J. Chem. Theory Comput.*, **2013**, 9, 3878-3888.
(4) D. S. C. D.A. Case, T.E. Cheatham, III, T.A. Darden, R.E. Duke, T.J. Giese, H. Gohlke, A.W. Goetz, D. Greene, N. Homeyer, S. Izadi, A. Kovalenko, T.S. Lee, S. LeGrand, P. Li, C. Lin, J. Liu, T. Luchko, R. Luo, D. Mermelstein, K.M. Merz, G. Monard, H. Nguyen, I. Omelyan, A. Onufriev, F. Pan, R. Qi, D.R. Roe, A. Roitberg, C. Sagui, C.L. Simmerling, W.M. Botello-Smith, J. Swails, R.C. Walker, J. Wang, R.M. Wolf, X. Wu, L. Xiao, D.M. York and P.A. Kollman, **2017***, AMBER 2017, University of California, San Francisco.*
(5) J. Wang, R. M. Wolf, J. W. Caldwell, P. A. Kollman and D. A. Case, *J. Comput. Chem.*, **2004**, 25, 1157-1174.
(6) C. I. Bayly, P. Cieplak, W. Cornell and P. A. Kollman, *J. Phys. Chem.*, **1993**, 97, 10269-10280.
(7) B. H. Besler, K. M. Merz and P. A. Kollman, *Journal of Computational Chemistry*, **1990**, 11, 431-439.
(8) U. C. Singh and P. A. Kollman, *J. Comput. Chem.*, **1984**, 5, 129-145.
(9) G. W. T. M. J. Frisch, H. B. Schlegel, G. E. Scuseria, M. A. Robb, J. R. Cheeseman, G. Scalmani, V. Barone, G. A. Petersson, H. Nakatsuji, X. Li, M. Caricato, A. Marenich, J. Bloino, B. G. Janesko, R. Gomperts, B. Mennucci, H. P. Hratchian, J. V. Ortiz, A. F. Izmaylov, J. L. Sonnenberg, D. Williams-Young, F. Ding, F. Lipparini, F. Egidi, J. Goings, B. Peng, A. Petrone, T. Henderson, D. Ranasinghe, V. G. Zakrzewski, J. Gao, N. Rega, G. Zheng, W. Liang, M. Hada, M. Ehara, K. Toyota, R. Fukuda, J. Hasegawa, M. Ishida, T. Nakajima, Y. Honda, O. Kitao, H. Nakai, T. Vreven, K. Throssell, J. A. Montgomery, Jr., J. E. Peralta, F. Ogliaro, M. Bearpark, J. J. Heyd, E. Brothers, K. N. Kudin, V. N. Staroverov, T. Keith, R. Kobayashi, J. Normand, K. Raghavachari, A. Rendell, J. C. Burant, S. S. Iyengar, J. Tomasi, M. Cossi, J. M. Millam, M. Klene, C. Adamo, R. Cammi, J. W. Ochterski, R. L. Martin, K. Morokuma, O. Farkas, J. B. Foresman, and D. J. Fox, *Inc.: Wallingford, CT*, 2009.
(10) P. Li, K. M. Merz, *J. Chem. Inf. Model.* **2016**, 56, 599−604.suscat
(11)
(12) J. A. Maier, C. Martinez, K. Kasavajhala, L. Wickstrom, K. E. Hauser and C. Simmerling, *J. Chem. Theory Comput.*, **2015**, 11, 3696-3713.
(13) T. Darden, D. York and L. Pedersen, *J. Chem. Phys.*, **1993**, 98, 10089-10092.
(14) Palatinus, L. & Chapuis, G. SUPERFLIP - a computer program for the solution of crystal structures by charge flipping in arbitrary dimensions. *J. App. Cryst.* **2007**, 40, 786-790.
(15) Sheldrick, G. A short history of SHELX. *Acta Cryst.* **2008**, A64, 112-122.